R-08-125

Feasibility study of a Single Well Injection Withdrawal (SWIW) experiment with synthetic groundwater

Rune Nordqvist, Johan Byegård, Calle Hjerne
Geosigma AB

Augusti 2008

Svensk Kärnbränslehantering AB
Swedish Nuclear Fuel
and Waste Management Co
Box 250, SE-101 24 Stockholm
Tel +46 8 459 84 00

ISSN 1402-3091
SKB Rapport R-08-125

Feasibility study of a Single Well Injection Withdrawal (SWIW) experiment with synthetic groundwater

Rune Nordqvist, Johan Byegård, Calle Hjerne
Geosigma AB

Augusti 2008

Abstract

This report describes the performance and results of a feasibility study regarding SWIW (Single Well Injection Withdrawal) tests with synthetic groundwater. The objectives of the study were to investigate the possibility to perform, analyse and evaluate SWIW tests with synthetic groundwater.

SWIW tests with synthetic groundwater imply that water similar to the natural groundwater is produced but without one or several compounds that naturally occurs in the groundwater. The synthetic groundwater is injected into the rock formation and later pumped back. The increase of the naturally occurring compounds may be analysed and provide information about diffusion processes in the rock formation.

Simulations of SWIW tests with synthetic groundwater shows that a combination of tests with and without a waiting period may provide good opportunities to distinguish between fast and slow diffusion processes, i.e. diffusion from stagnant zones and rock matrix. Furthermore, the simulations show that it is important to use many tracers with different characteristics regarding diffusion and sorption in order to facilitate the evaluation. If additional boreholes exist in the vicinity that may be used as observation holes for tracer breakthrough, it would be a great benefit for the evaluation of the tests.

This study shows that it is possible to produce a synthetic groundwater of sufficient amount and purity to a reasonable cost at CLAB (Baslab).

The starting point for the study was to use the test site TRUE Block Scale in the Äspö tunnel. The study shows that the well characterized structures #19 and #20 probably had been suitable for SWIW tests. However, during the feasibility study a project started that will result in a new tunnel in the vicinity of TRUE Block Scale. This implies that the site will not be accessible for experiments until 2009 at the earliest. The new tunnel may also change the hydraulic characteristics at the site so that it is no longer suitable for SWIW tests. Hence, other sites for SWIW tests with synthetic groundwater should be considered. The test site should be well characterised, have a low hydraulic gradient and not have any high hydraulic conductivity features in the vicinity.

Sammanfattning

Denna rapport beskriver genomförandet och resultaten av en förstudie angående SWIW-test (Single Well Injection Withdrawal test) med syntetiskt grundvatten. Förstudiens syfte är att undersöka möjligheterna att genomföra, analysera och utvärdera SWIW-test med syntetiskt grundvatten.

SWIW-test med syntetiskt grundvatten innebär att vatten likt det naturliga grundvattnet men utan ett eller flera naturligt förekommande ämnen tillverkas. Det syntetiska grundvattnet injiceras i bergformationen och pumpas sedan tillbaka. Ökningen av de naturligt förekommande spårämnena i det tillbakapumpade vattnet kan sedan analyseras och ge information om dominerande diffusionsprocesser i spricksystemet.

Simuleringar av SWIW-test med syntetiskt grundvatten visar att en kombination av test med och utan vänteperiod ger goda möjligheter att skilja på snabba och långsamma diffusionsprocesser, dvs diffusion från stagnanta zoner respektive bergmatrisen. Vidare visar simuleringarna att det är viktigt att använda många spårämnen med olika egenskaper med avseende på diffusion och sorption för att underlätta tolkningen. Om det finns ytterliggare borrhål i närheten som kan användas som observationshål för spårämnesgenombrott skulle det vara en stor fördel för detta experiment.

Denna studie visar att det är möjligt att tillverka ett syntetiskt grundvatten med lämpliga koncentrationer av olika ämnen till en rimlig kostnad på CLAB (Baslab).

Utgångspunkt för studien var att använda experimentplatsen TRUE Block Scale i Äspötunneln. Studien visar att de väl kartlagda strukturerna #19 och #20 troligen hade varit lämpliga som försöksplats för SWIW-test. Under förstudiens gång startade emellertid ett projekt som innebär att en ny tunnel drivs i närheten av TRUE Block Scale vilket gör att platsen inte blir tillgängligt för experiment förrän tidigast i början av 2009. Den nya tunneln kan dessutom innebära att de hydrauliska förhållandena förändras i TRUE Block Scale signifikant så att platsen inte längre är lämplig för SWIW-test. Därför bör man överväga att utföra SWIW med syntetiskt grundvatten på en annan plats i Äspö-tunneln. Experimentplatsen bör vara välkarakteriserad, ha en låg hydraulisk gradient i målstrukturen och inte ha några högkonduktiva hydrauliska strukturer i närheten.

Contents

1 Introduction

Single Well Injection Withdrawal tests (SWIW, sometimes also referred to as “Push-pull” tests) have been used frequently in the site investigations at Forsmark and Oskarshamn with the objective to demonstrate and investigate transport properties in fractures. In a typical SWIW test, one or more tracers are added to the injection water (consisting of natural groundwater sampled prior to the injections) and the tracer breakthrough during the recovery/pumpback phase is evaluated. In a SWIW test with synthetic groundwater, on the other hand, a synthetic groundwater is prepared and used in the injection phase that lacks one or more of the natural salt components (e.g. chloride, potassium, strontium). This type of experiment addressing the out-diffusion from at saturated rock is foreseen /e.g. Haggerty 1999/ to better facilitate studies of the diffusion characteristics in fractured rock than a normal SWIW test. Furthermore, in order to obtain a comparison with the tracer technique normally used in the SWIW tests it is beneficial if a set of non-sorbing and sorbing tracers are added in the injection phase of the experiment.

The idea is that the information about diffusion characteristics will be obtained by comparing the breakthrough curves for e.g. chloride, potassium, strontium and the added tracers. If the process of diffusion in the stagnant water is dominating, the increase of the ions should be possible to explain from the diffusivity in water. On the other hand, if the diffusion in the rock matrix is dominating, the increase should be much slower (i.e. determined by the rate of the much slower pore diffusion). One may also presume that diffusion from stagnant water will give relative concentration increase in the withdrawal water that will be more or less independent whether the tracer is sorbing or non-sorbing which will not be the case if pore diffusion is the major mechanism.

Radon-222 ($t_{½}$=3.8 d) is a radioactive non-sorbing tracer which is produced from the decay of Ra-226 ($t_{½}$=1,600 y) in the rock matrix. It is assumed that it reaches the groundwater by diffusion from the rock pores to the fractures. Since this tracer therefore is continuously produced from the rock matrix, it will not be depleted to the same extent as the other tracers. Therefore, the breakthrough characteristics of this tracer will be different and could possibly provide distinct information of the extent of the diffusion from the rock matrix. Furthermore, estimations of the fracture aperture could be obtained from the radon concentrations combined with laboratory data for radon flux, as described in /Byegård et al. 2002/. Hence, it is furthermore an advantage that a synthetic groundwater used in the SWIW test which, opposite to natural sampled groundwater, easily can be prepared free of radon.

Since the matrix diffusion is presumed to be a very slow process, it must be acknowledged that there might be difficulties to obtain a distinct matrix diffusion signal in a SWIW experiment with limited duration. The possibility of being able to distinguish the processes described above must therefore be tested by doing scoping calculations as is presented in this study.

2 Objectives

The objectives of this study are to evaluate the possibility to perform and analyze a SWIW test with synthetic groundwater at the TRUE-Block Scale site and to optimize such a test, including pre-tests, with respect to test site, test performance and evaluation. The report will focus on the following objects:

- A summary of the knowledge of the hydraulic properties of the TRUE Block Scale experiment site.
- Scoping and design calculation in order to investigate the possibilities to do experiments which will produce breakthrough curves from which the diffusion processes (e.g. rock matrix diffusion and/or diffusion into stagnant pores) can be verified and quantified.
- Scoping and design calculations in order to investigate the possibilities of obtaining breakthrough curves from which the sorption parameters (e.g. K_d) can be quantified.
- Investigation of the possibilities to produce synthetic groundwaters with such a low content of the natural groundwater components (e.g. chloride, sodium, calcium) that a quantification can be made of the diffusion of theses species from the matrix pore water to the synthetic groundwater.
- Investigation of the possibilities to use radon as a tracer to quantify the fracture aperture, a parameter which is necessary in order to be able to evaluate the diffusivities and the sorption parameters from the breakthrough curves.
- Estimation of the costs for a proposed experiment.

3 Scope

Several aspects of the feasibility to perform and evaluate a SWIW test with synthetic groundwater at TRUE-Block Scale were analyzed in this study. Hence, a number of methods were used. Some of them require a short description which follows.

3.1 Hydraulic properties of TRUE Block Scale

In order to evaluate the hydraulic properties of TRUE Block Scale (TRUE-BS) information was gathered from HMS, SICADA and various reports. This study of TRUE-BS focuses on two different structures, #19 and #20, which have been extensively investigated in earlier projects.

The coordinates of the borehole intercepts with structures #19 and #20 were interpolated from the intercept (borehole length) listed in earlier reports and the borehole coordinates on both sides of each intercept (from SICADA). These intercept coordinates were transformed numerically in order to produce plots with a view perpendicular to the structure. However, since the intercepts for each structure are not in one plane exactly, the internal distances in the plot may not be exactly as the true distances. Still, the internal distances in the plots are very close to the true distances.

The hydraulic head at different times was interpolated (Kriging) between the borehole intercepts in the structures and plotted in order to evaluate the change of the hydraulic gradient in the structure. At the times chosen for these plots, the hydraulic head in TRUE-BS were considered to not be affected by any extraordinary events.

3.2 Experience

Experience from earlier SWIW tests, both underground and from the surface, as well as experiences from tracer tests in TRUE-BS was gathered by reading reports and by interviewing experienced persons within these fields.

3.3 Scoping simulations and design calculations

The scoping simulations were carried out using SUTRA /Voss 1984/, a numerical simulation code for flow and transport developed at the USGS (United States Geological Survey). Simulations of the various experimental phases were performed assuming steady state flow and transient solute transport. The following experimental phases were included in the simulations:

1) water injection phase,
2) waiting phase (for some of the simulations),
3) recovery (pump-back) phase.

All of the simulations were performed in a radial symmetry, with the innermost nodes located at the borehole wall (i.e. at a distance equal the borehole radius) and the outermost nodes located at a sufficiently distant boundary to prevent interference of boundary effects on simulation results.

The boundary condition at the innermost nodes was steady-state flow, while the outermost nodes were assigned a constant value of hydraulic head. For the waiting phase, the flow at the well nodes is specified to zero effectively creating a no-flow boundary. This may not be entirely realistic as back-diffusion of solute into the borehole should be possible to occur during the waiting phase; this process would not be accounted for by the simulation model during a waiting phase.

The hypothesized experiment is in this case "reversed" since the solutes to be investigated would not be introduced into the fracture system during the injection phase. Instead, the solutes in the formation are expected to mix into the synthetic injection water. Accordingly, an initial condition for the simulations is that all nodes are assigned a specified concentration value.

The radial distance to the outermost nodes was set to 40 metres and the borehole radius (r_w) to 0.038 m (i.e. a borehole diameter of 76 mm). The extent of the matrix was 0.2 m from the centre of the fracture. In the fracture, the porosity was set to 1 while the matrix porosity was set to a value of 1×10^{-3}.

Sorption of tracers was simulated by assuming a value for the linear equilibrium sorption coefficient (K_d) in the matrix. This value was set to 1×10^{-3} m^3/kg, which gives a relatively strong sorption effect when combined with other parameters defined below. The density of the solid rock was set to 2,500 kg/m^3. The longitudinal dispersivity (a_L) was set to 0.25 m, which is intended to represent a relatively small dispersivity value and also within reasonable bounds for what may be expected from a SWIW test based on experience from the SKB site investigation programmes /Nordqvist 2007/. The effect of dispersion on SWIW breakthrough curves are illustrated and briefly discussed in section 4.3.

Four simple fracture configurations were used:

1. Single fracture without matrix (i.e. a one-dimensional homogenous radial model); in the simulation model the fracture aperture is set to 2×10^{-4} m. The aperture value is chosen somewhat arbitrary but, based on the cubic law, corresponds to transmissivity values in fractures typically used for SWIW experiments within the site investigations.
2. Single fracture with a high-porosity (porosity set to 1) stagnant zone. This was accomplished by adding a 4×10^{-4} m (0.4 mm) thick layer to each side of the flowing fracture. This value is somewhat arbitrary and only intended to be large enough to show typical effects of such zones.
3. Single fracture with porous stagnant rock matrix, shown in Figure 3-1; the value of matrix porosity is set to 1×10^{-3}.
4. Single fracture with porous rock matrix and a stagnant water zone. This was done by inserting a high-porosity (porosity set to 1) stagnant zone, of the same thickness as in 2 above, between the flowing fracture and the matrix. This is the only simulated variant including a high-porosity stagnant zones and low porosity rock matrix simultaneously, which is a limitation of this study as other combinations of stagnant zones and matrix are possible as well.

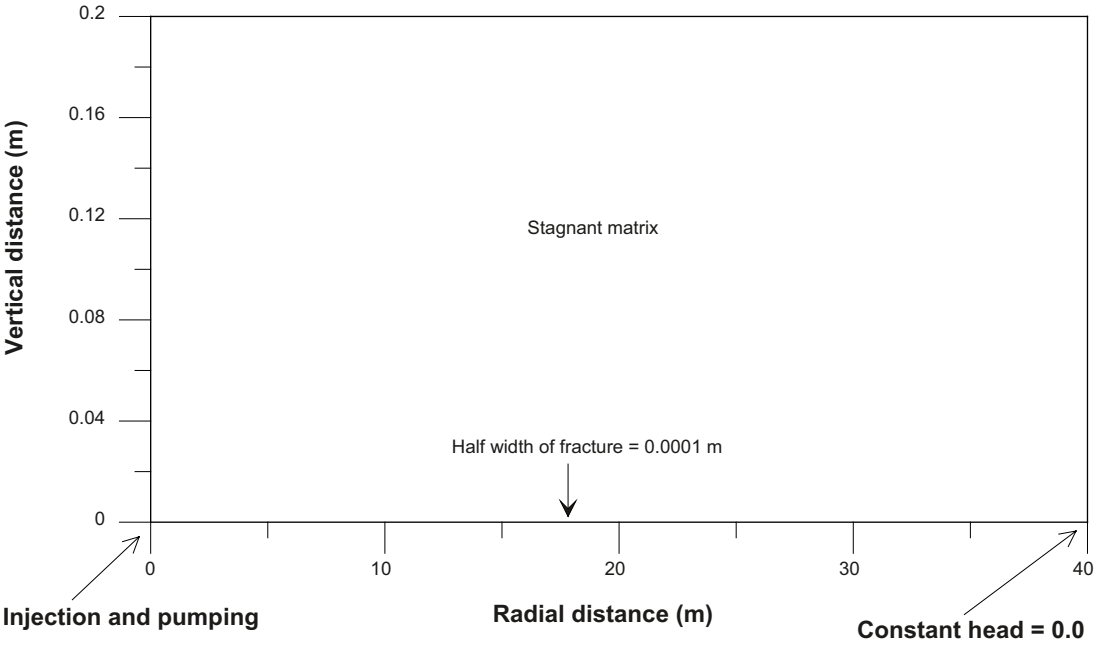

Figure 3-1. *Simulation geometry for the case of a single fracture with a stagnant matrix.*

The simulation code is based on the finite-element method. The sizes of the elements must be carefully designed in order to obtain representative results. For these simulations, element sizes start very small closest to the borehole and expand with distance. The first element closest to the borehole is about 0.1 mm. In the vertical direction, the fracture is divided into ten elements (i.e. 0.01 mm). In the matrix, element sizes increase somewhat with distance from the flowing fracture. There may be some discretisation effects at the narrow interface zone (on the order of less than 0.1 mm) where the fracture gradually becomes the matrix. For strongly sorbing tracers, this interface zone may have some impact on the simulated results. In order to simulate an ideal dual-porosity system completely accurately, finer discretisation may be needed, although this would require much longer simulation times. However, despite possible discretization effects at the interface, it should be possible to obtain general features of the planned experiment under various experimental set-ups.

The SWIW simulations were carried out with a tracer injection period of about 2.6 hours with a flow rate of about 14.4 L/h (4×10^{-6} m^3/s). This gives a total injected volume of about 37.4 L, which gives a suitable radial travel distance in the simulation model of about 7.7 m. The waiting period, when employed, was set to 48 hours. The durations of the various simulated phases are intended to be relatively short because it is anticipated that the proposed experiment may be carried out in the vicinity of a tunnel and that loss of tracer due to high flow gradients may be of concern. The choices of simulation flows and durations are generally based on typical experimental designs for SWIW test within the site investigation programmes.

The primary result from the scoping calculations is the tracer breakthrough curve in the SWIW borehole during the recovery pumping phase, because this will also be the main experimental result. The simulation output represents tracer concentrations at the borehole/fracture interface under ideal conditions. Experimental data, on the other hand, will be affected to various extents by mixing processes in the borehole section. During the tracer injection phase, the water in the borehole section is continuously stirred. Although this will modify an otherwise rectangular injection pulse somewhat, it will likely not have any significant effects on the resulting tracer recovery curve. During the recovery pumping phase, pumping will probably be carried out without continuous mixing in the borehole section. Therefore it should be reasonable to expect some initial dilution/mixing effects at the very beginning of the tracer breakthrough curve. This may be an important consideration in cases where the early parts of the recovery breakthrough

may be important for analysis and interpretation. As a rough estimate of the time required before water is pumped from the tested fracture, one may consider a 1 m borehole section with a dummy that results in 3 mm slot as the effective experimental borehole volume. With the assumed pumping flow of 14.4 l/h, it would, at the most, take about 6 minutes before water from the tested fracture would start entering the sampling tubing inlet.

The above comments about experimental borehole effects are based on the assumption that available SWIW test equipment is used and that the same experimental procedure as during the site investigations is employed.

3.4 Production of synthetic groundwater

As described above, the basic idea of this experiment is to perform a SWIW test with injection of water free from the normal main components in the groundwater (i.e. Na, Ca and Cl). During the withdrawal phase the diffusion rate of these components from the matrix and stagnant zones into the injection water will be studied.

The concept used for this proposed work consist of the absence of these major components in the injected groundwater should be compensated by the introduction of analogous elements in the same molar concentration, i.e.;

- The absence of Cl^- should be compensated by introduction of NO_3^-.
- The absence of Na^+ should be compensated by introduction of Li^+.
- The absence of Ca^{2+} should be compensated by introduction of Mg^{2+}.

The reason for doing this and not to just use deionised water is mainly to avoid obtaining ion strength gradients between the injected and the natural groundwater. Furthermore, if an ion strength gradient is considered for a matrix diffusion process, the diffusion migration of a nonsorbing anionic tracer will have to be followed by a simultaneous migration of a cationic tracer, this since a electrical neutrality has to maintained. The outcome of this will be a reduced diffusion rate for the non-sorbing tracer since the rate will be determined from the diffusion rate of their accompanying sorbing cations. Avoiding or minimizing any chemical gradients of this kind will enable matrix diffusion of non-sorbing anion to take place with a spatial exchange mechanism, e.g. an exchange of Cl^- towards NO_3^- without a simultaneous migration of a Na^+ necessary to take place.

In order to evaluate the possibilities to manufacture synthetic groundwater in sufficient amount and quality, chemical data from earlier reports, the purity of de-ionized water and the cost of the chemicals were considered.

4 Results

4.1 Hydraulic properties of TRUE Block Scale

4.1.1 Structure #19

Table 4-1. Borehole intercept with #19.

Borehole	Intercept with #19 Borehole length (m) [a]	Northing (m) [b]	Easting (m) [b]	Elevation (m) [b]
KA2563A	238.0	7,179.00	1,873.57	–498.78
KI0023B	111.7	7,154.70	1,893.75	–487.58
KI0025F	166.7	7,081.41	1,935.37	–501.43
KI0025F02	133.0	7,124.42	1,912.20	–503.58
KI0025F03	124.7	7,141.75	1,902.99	–509.00

[a] /Andersson et al. 2002a/

[b] Interpolated (coordinate system ÄSPÖ96)

Table 4-2. Distances between borehole intercepts in #19 (m).

Borehole	KA2563A	KI0023B	KI0025F	KI0025F02	KI0025F03
KA2563A		33.5	115.5	67.0	48.6
KI0023B	33.5		85.4	38.9	26.7
KI0025F	115.5	85.4		48.9	68.9
KI0025F02	67.0	38.9	48.9		20.4
KI0025F03	48.6	26.7	68.9	20.4	

As illustrated by the Figures 4-1, 4-2 and 4-3, the character of the hydraulic gradient has not changed much from September 2003 to present. It appears that the area around KI0025F03 has the lowest hydraulic head at all three times. However, it should be noted that the hydraulic head decreased from c. –42 m.a.s.l. to c. –54 m.a.s.l. during the period. It also appears that the hydraulic gradient is larger in the two later figures than the first. This is also visible in Table 4-3 below where the hydraulic gradients between the three boreholes in the centre of #19 are displayed.

The section volumes, including hoses, in the sections including structure #19 is in the range of 3–9 liters.

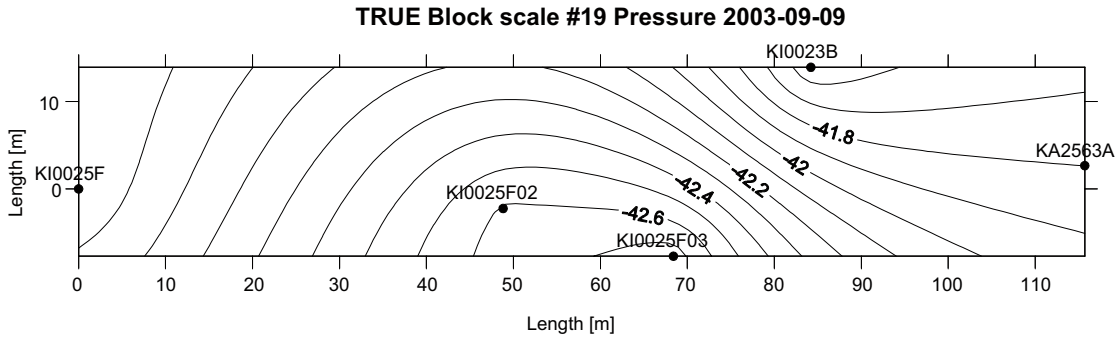

Figure 4-1. *Interpolated hydraulic head in #19 2003-09-09.*

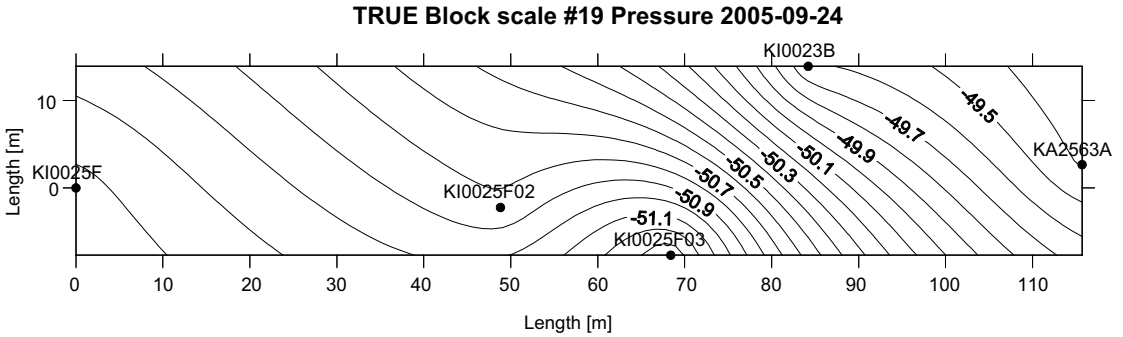

Figure 4-2 *Interpolated hydraulic head in #19 2005-09-24.*

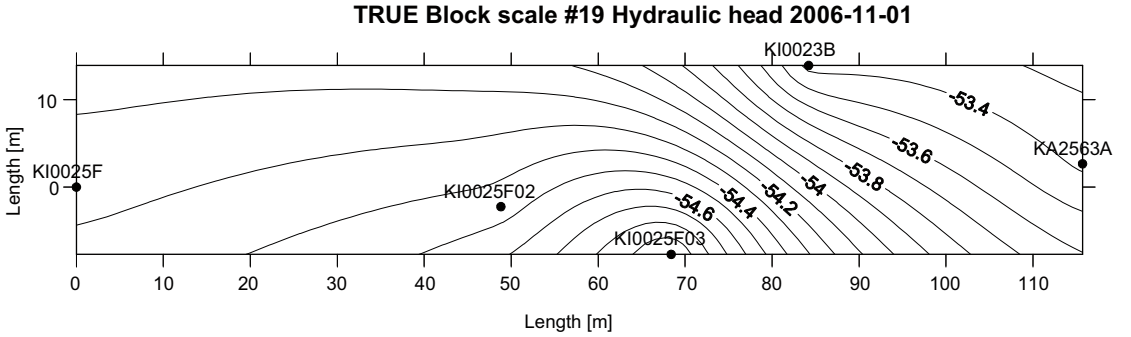

Figure 4-3. *Interpolated hydraulic head in #19 2006-11-01.*

Table 4-3. Hydraulic gradient between boreholes in #19.

Date	KI0023B-KI0025F02	KI0023B-KI0025F03	KI0025F02-KI0025F03
2003-09-09	0.0278	0.0459	0.0069
2005-09-24	0.0310	0.0664	0.0277
2006-11-01	0.0278	0.0619	0.0279

4.1.2 Structure #20

Table 4-4. Borehole intercept with #20.

Borehole	Intercept with #20 Borehole length (m) [a]	Northing (m) [b]	Easting (m) [b]	Elevation (m) [b]
KA2511A	122	7,153.25	1,936.72	–403.06
KA2563A	188.7	7,197.81	1,905.93	–466.70
KI0023B	69.8	7,187.30	1,915.30	–472.60
KI0025F	87.7	7,156.04	1,944.52	–477.30
KI0025F02	74.7	7,174.66	1,929.90	–479.89
KI0025F03	73.2	7,182.03	1,923.27	–484.15

[a] /Andersson et al. 2002a/

[b] Interpolated (coordinate system ÄSPÖ96)

Table 4-5. Distances between borehole intercepts in #20 (m).

Borehole	KA2511A	KA2563A	KI0023B	KI0025F	KI0025F02	KI0025F03
KA2511A		83.6	80.3	74.7	80.0	87.1
KA2563A	83.6		15.3	57.8	35.8	29.2
KI0023B	80.3	15.3		43.0	20.6	15.0
KI0025F	74.7	57.8	43.0		23.8	34.3
KI0025F02	80.0	35.8	20.6	23.8		10.8
KI0025F03	87.1	29.2	15.0	34.3	10.8	

The character of the hydraulic gradient in feature #20 has been rather stable during the studied time period. This is easily observed in Figures 4-4, 4-5 and 4-6 as the lower hydraulic heads are found in the central part of the feature (KI0023B and KI0025F02) and higher hydraulic heads are found on either side. However, it should be noted that the hydraulic head decreased from c. –45 masl to c. –58 masl during the period. The development of the gradients has been different in the structure. For example, as seen in Table 4-6, it has increase between KA2563A and KI0023B while it has decreased between KI0023B and KI0025F02.

The section volumes, including hoses, in the sections including structure #20 is in the range of 4–7 liters, except for KI0023B which is close to 14 liters.

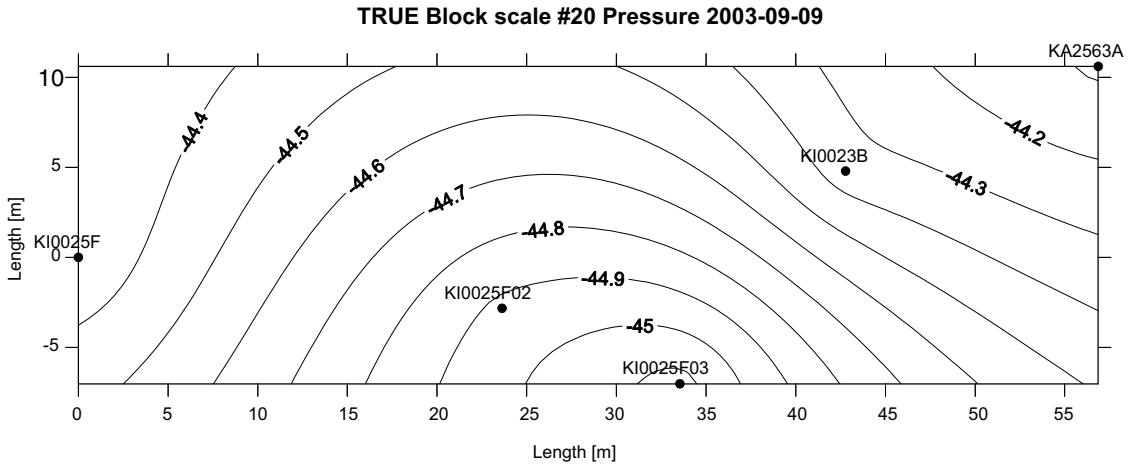

Figure 4-4. *Interpolated hydraulic head in #20 2003-09-09.*

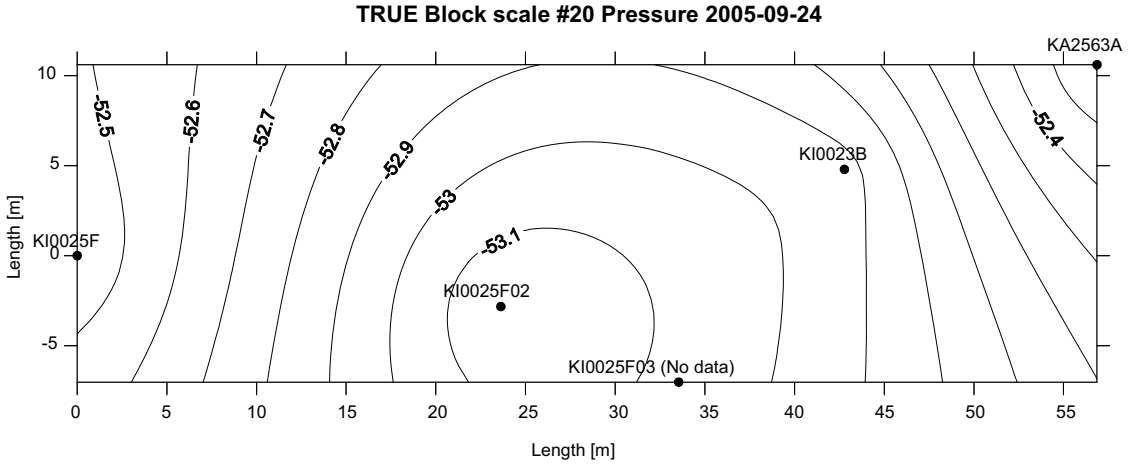

Figure 4-5. *Interpolated hydraulic head in #20 2005-09-24.*

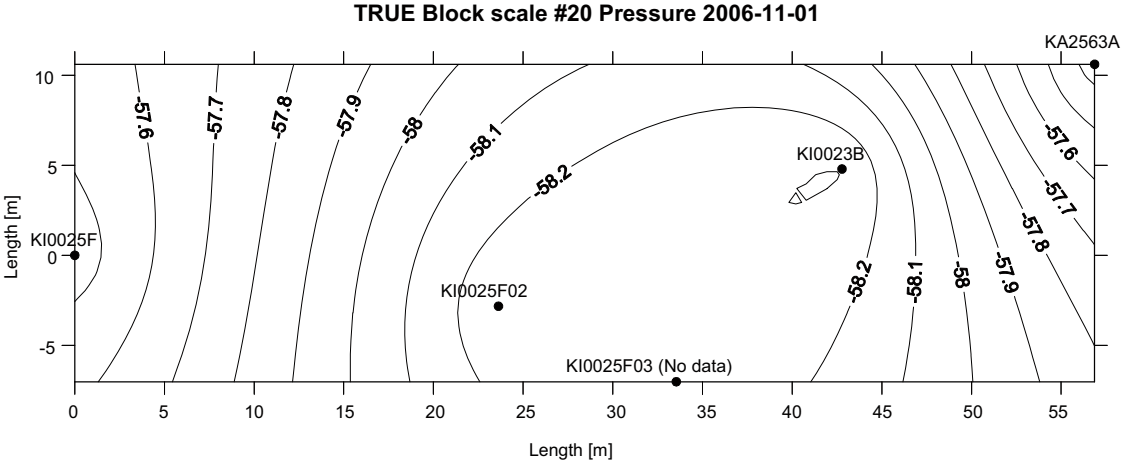

Figure 4-6. *Interpolated hydraulic head in #20 2006-11-01.*

Table 4-6. Hydraulic gradient between boreholes in #20

Date	KA2563A-KI00023B	KI0023B-KI0025F02	KA2563A-KI0025F02
2003-09-09	0.0172	0.0281	–0.0235
2005-09-24	0.0494	0.0122	–0.0281
2006-11-01	0.0626	–0.0013	–0.0259

4.2 Experience

4.2.1 Structure #19

A number of tests called CPT, as presented by /Andersson et al. 2004/, was earlier performed in #19. These tests showed that KI0025F03:R3 was suitable as a sink in cross-hole tracer tests. Furthermore, these tests also showed that a high recovery (> 80%) was possible to obtain when injecting a tracer in KI0025F02:R3. Other sections in #19 used for injection that resulted in a relatively good recovery in KI0025F03:R3 was KI0023B:P2 and KA2563A:S1. The latter was however, uncertain due to degradation of the tracer during the experiment.

4.2.2 Structure #20

Earlier studies, presented by /Andersson et al. 2002b/, show that it is possible to obtain a high recovery during tracer tests in #20. Two flow paths in particular display a very high recovery (100%), from KI0025F02 to KI0035F03 and from KI0025F03 to KI0023B. The flow paths from KA2563A to KI0023B and KI0025F03 and from KI0025F02 to KI0023B displayed recoveries of about 50%. However, in KI0023B there exists a hydraulic short-circuit between sections P6 and P7 which could make it less favorable as injection hole for tracers in #20.

4.2.3 Earlier SWIW tests

SWIW tests have previously been performed within the ongoing site investigations in Forsmark and Laxemar. Two SWIW tests have also been performed at the TRUE-1 site.

In general, the SWIW tests within the site investigations have resulted in a rather high recovery (> 80%) for the non-sorbing tracer uranine. Regarding the sorbing tracer cesium, which also has been used extensively, the recovery for a majority of the tests has been about 50%. The hydraulic gradient during these tests has been estimated by the means of dilution tests and often been rather low (a few percent).

At the TRUE-1 site two SWIW tests has been performed in KXTT4, Feature A. The recovery of the tests was rather low (< 10%) for a non-sorbing tracer. One possible explanation of the low recovery is the presence of a highly conductive feature in the influence area of the tests that may have transported the tracer too far away from the test section before the pumping phase. It should be pointed out that Feature A at the TRUE-1 site is only c. 15 m from the tunnel wall which may have contributed to the low recovery in the tests. In these tests the tracer breakthrough was monitored in some surrounding boreholes by passive sampling which turned out to provide important information for the evaluation of the test.

4.3 Scoping simulations and design calculations

4.3.1 Simple 1-D fracture

This example comprises the simplest possible radial flow and transport geometry in order to illustrate the “reverse” tracer breakthrough (the term “tracer breakthrough” will be used herein despite that it actually is “water breakthrough”) resulting from injection of solute-free water. Figure 4-7 shows tracer breakthrough at four different radial distances: the borehole radius (r_w), 3,5 and 8 m.

In the example in Figure 4-7, the solute initially present throughout the fracture becomes replaced with solute-free water injected during the first phase of the SWIW test. At the most remote distance in the plot (8 m), the fracture solute is only partially replaced before the time of flow reversal.

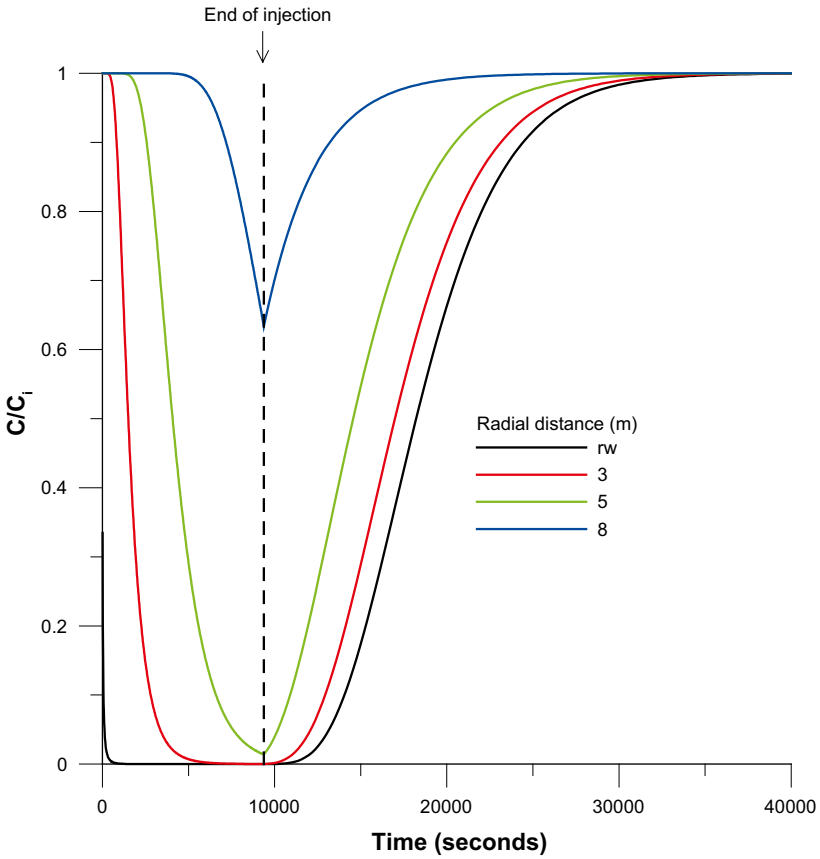

Figure 4-7. *Illustration of solute-free water breakthrough in a single fracture assuming radial flow and transport.*

The behaviour of sorbing tracers in a single flowing fracture is illustrated in Figures 4-8 and 4-9. In this case, sorption is simulated by setting a retardation factor for the flowing fracture. Figure 4-8 shows tracer breakthrough in the tested SWIW section (at $r = r_w$) for several different retardation factors. Because flow and transport is reversed during the pumping phase, the visible differences between tracers with different retardation factors are relatively small compared to tracer breakthrough in cross-hole tracer tests. This is illustrated in Figure 4-9, where the breakthrough at a radial distance of 3 m is plotted. Here only the sorbing tracer with the lowest retardation factor (of the ones shown in Figure 4-8) is affected; the more sorbing tracers (not shown in Figure 4-9) are not affected at all at this travel distance.

Dispersion effects

The effect of hydrodynamic dispersion on the tracer recovery curve is illustrated in Figure 4-10, where breakthrough curves for three different dispersivities are shown.

Figure 4-10 shows that varying the dispersion parameter may give similar results as varying the fracture retardation factor for sorbing tracers as shown in Figure 4-8. Dispersion effects may in some cases also be similar to diffusion effects as may be seen from some of the results shown in subsequent sections. Although dispersion effects may be similar to other effects, it is assumed that transport process identification primarily will be attempted through comparison of tracers with different properties. Any dispersive effects are assumed to be equally "experienced" by all of the tracers, although this may not necessarily be the case for sorbing tracers vs. non-sorbing tracers.

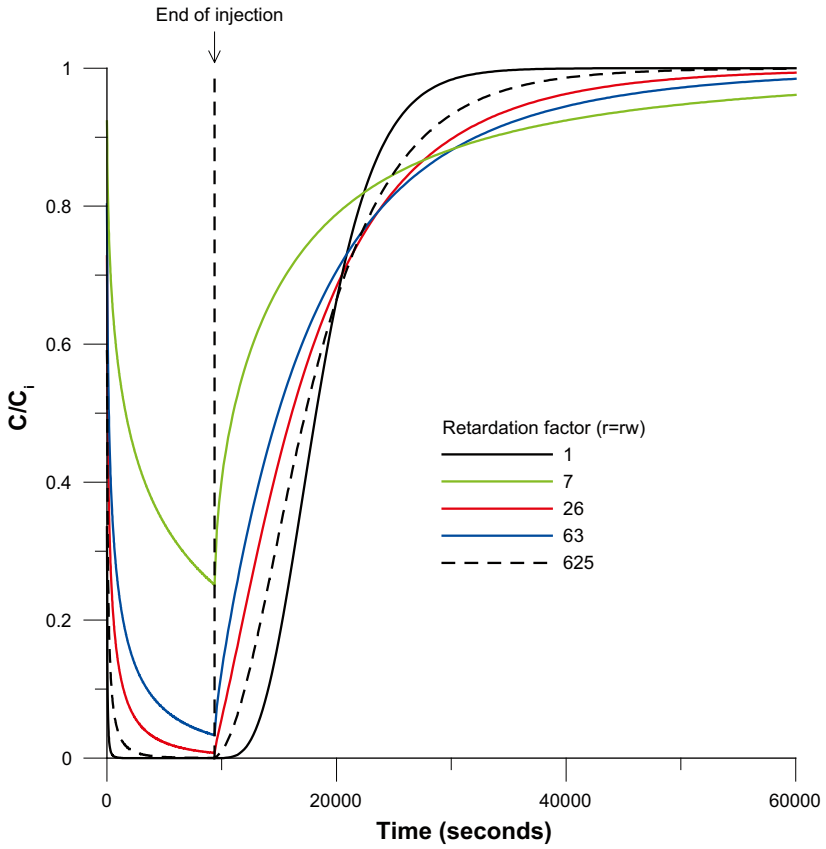

Figure 4-8. *Illustration of simulated breakthrough of sorbing tracers in the SWIW borehole section.*

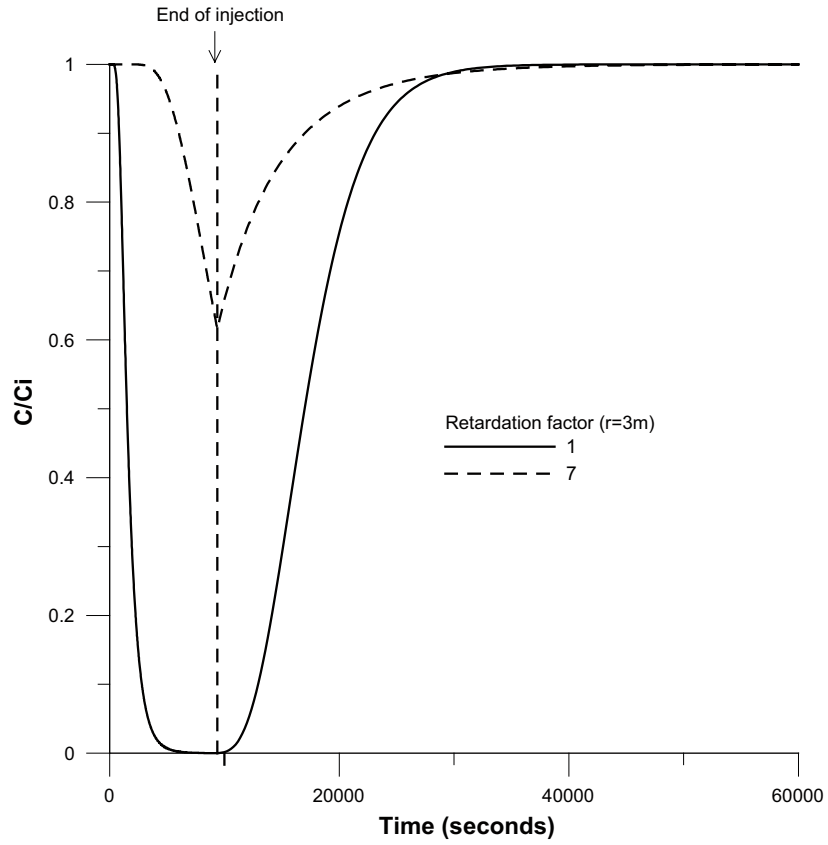

Figure 4-9. *Simulated breakthrough of a moderately sorbing tracer at a radial distance of 3 m.*

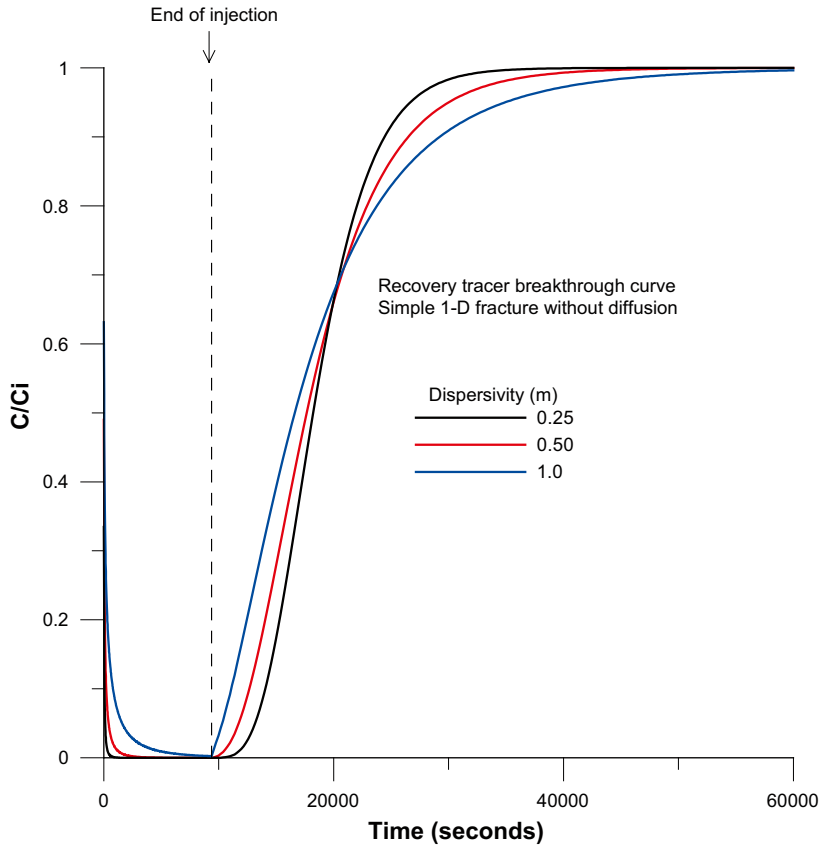

Figure 4-10. *Effect of dispersion on the tracer recovery breakthrough curve in the SWIW borehole section.*

4.3.2 Single fracture with matrix diffusion and non-sorbing tracers

These simulations correspond to geometrical case 3 listed above. Although individual values of various transport parameters are set in the simulation model, they are not independent. Instead, effective parameters may be defined. In a system with a flowing fracture and a porous matrix, an effective parameter that contains the matrix diffusion effect may be defined as /Moreno et al. 1983/:

$$A = \frac{\delta}{2 p_m \sqrt{R_d D_p}} \qquad \text{(Equation 4-1)}$$

where δ is the fracture aperture [L], p_m is the matrix porosity [–], D_p is the pore diffusivity [L^2/T] and R_d is a matrix retardation coefficient defined as:

$$R_d = 1 + \frac{1 - p_m}{p_m} \rho_s K_d \qquad \text{(Equation 4-2)}$$

where ρ_s is the density of the solid rock [M/L^3] and K_d is the linear equilibrium sorption coefficient [L^3/M^3].

Figure 4-11 shows the simplest case with non-sorbing tracers in a single fracture, matrix diffusion and no waiting period. The different cases in Figure 4-11 are denoted in two ways. First, by specifying a value of the pore diffusivity (D_p), given that other coupled parameters (δ = 0.2 mm, ρ_s = 2,500 kg/m^3, $p_m = 1 \times 10^{-3}$) are fixed in the simulation model; the range of D_p values is relatively large, actually extending to higher values than what would be expected from literature values of diffusivity. Second, the corresponding values of A (Equation 4-1) are also given. Any combination of the individual parameters that gives the same value of A will give the same simulation results.

The simulated cases shown in Figure 4-11 are very similar, only very large diffusion effects give a slight effect compared with the case of no diffusion. This result is straight-forward and might be expected, given the relatively short time frame.

By adding a waiting period of 48 hours, the time available for diffusion is increased significantly compared with the case of no waiting period. Figure 4-12 shows the simulation results for the case with a waiting period. The top part of the figure shows the entire simulation sequence while the bottom part approximately shows the pumping (recovery) phase with the same x-axis resolution as in Figure 4-11 and all other plots with no waiting period employed. For the most part of the tracer breakthrough curve, there are still no dramatic differences between varying degrees of matrix diffusion effects. The exception is the early parts of the curves, where increasing diffusion effects result in higher starting values for the tracer recovery curve. This would be caused by back-diffusion towards the borehole during the waiting phase. One may note that the most significant differences occur during the waiting period from which sampling will not be possible during the actual field experiment.

4.3.3 Single fracture with matrix diffusion and sorbing tracers

Next, corresponding simulations, as in the preceding section, with relatively strong matrix sorption are shown. Figure 4-13 shows the case without waiting period and Figure 4-14 the case with a waiting period. Figures 4-13 and 4-14 shows more visible effects than for the corresponding case with non-sorbing tracer (see Figure 4-11). For less strongly sorbing tracers (such as Li and Mg), the effects would be expected to be less visible. One should comment here that effects of strong sorption in the matrix may look similar to moderate retardation factors in a single fracture without matrix diffusion (Figure 4-8).

The simulation results are in this case more complex than for preceding cases. For the higher diffusivity values, diffusion has clearly a major influence on simulated results. For lower diffusivity values, sorption close to the fracture/matrix interface has a more dominating influence on the shape of the breakthrough curve and those cases may be expected to more resemble the cases with single fracture sorption in Figure 4-8. However, if a waiting period is employed (Figure 4-14), the combination of sorption and diffusion shows effects that may not be possible with only equilibrium sorption in the fracture. The effects at lower diffusivity values are partly due to the discretised nature of the simulation model, which gives tracer in the flowing fracture access to some sorption capacity at the fracture/matrix interface even when there is little diffusion.

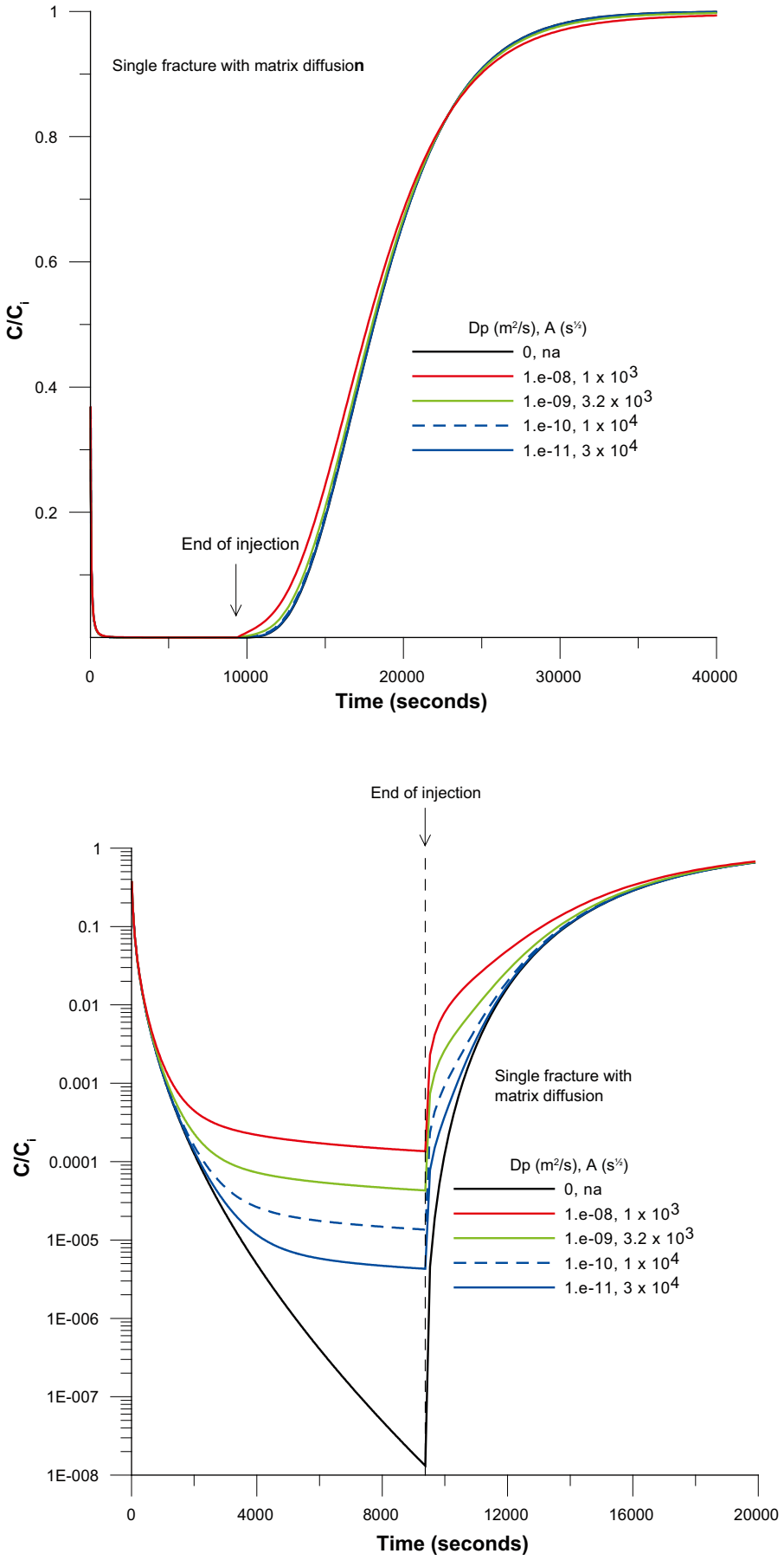

Figure 4-11. *Simulated breakthrough in the SWIW borehole section of non-sorbing tracers in a single fracture with matrix diffusion plotted in linear (top) and semi-logarithmic (bottom) scale. The matrix porosity is set to 1 x 10^{-3}.*

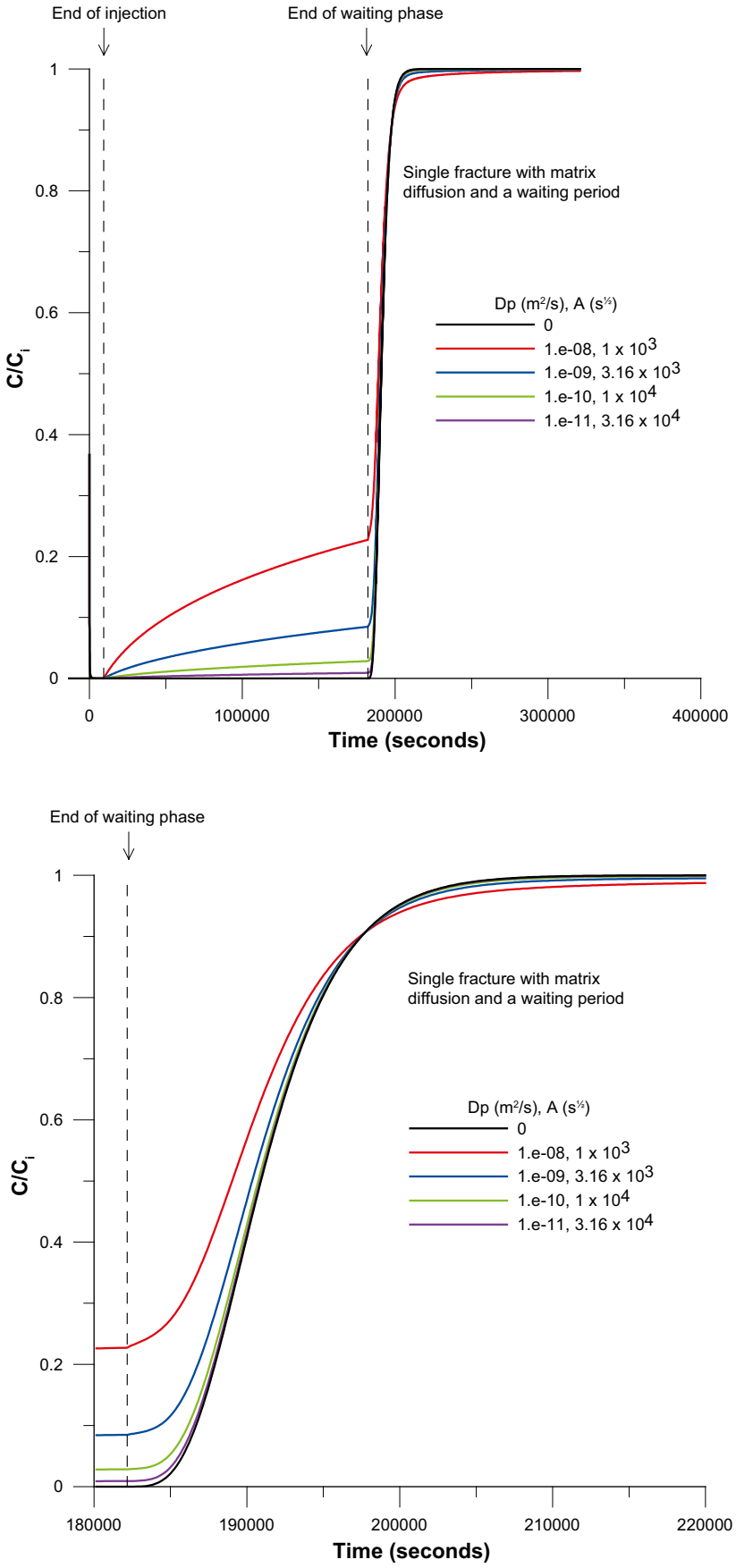

Figure 4-12. *Simulated breakthrough in the SWIW borehole section of non-sorbing tracers in a single fracture with matrix diffusion and a waiting period of 48 hours. The entire simulation sequence (top) is shown as well as a detailed plot of the recovery phase (bottom). The matrix porosity is set to 1 x 10⁻³.*

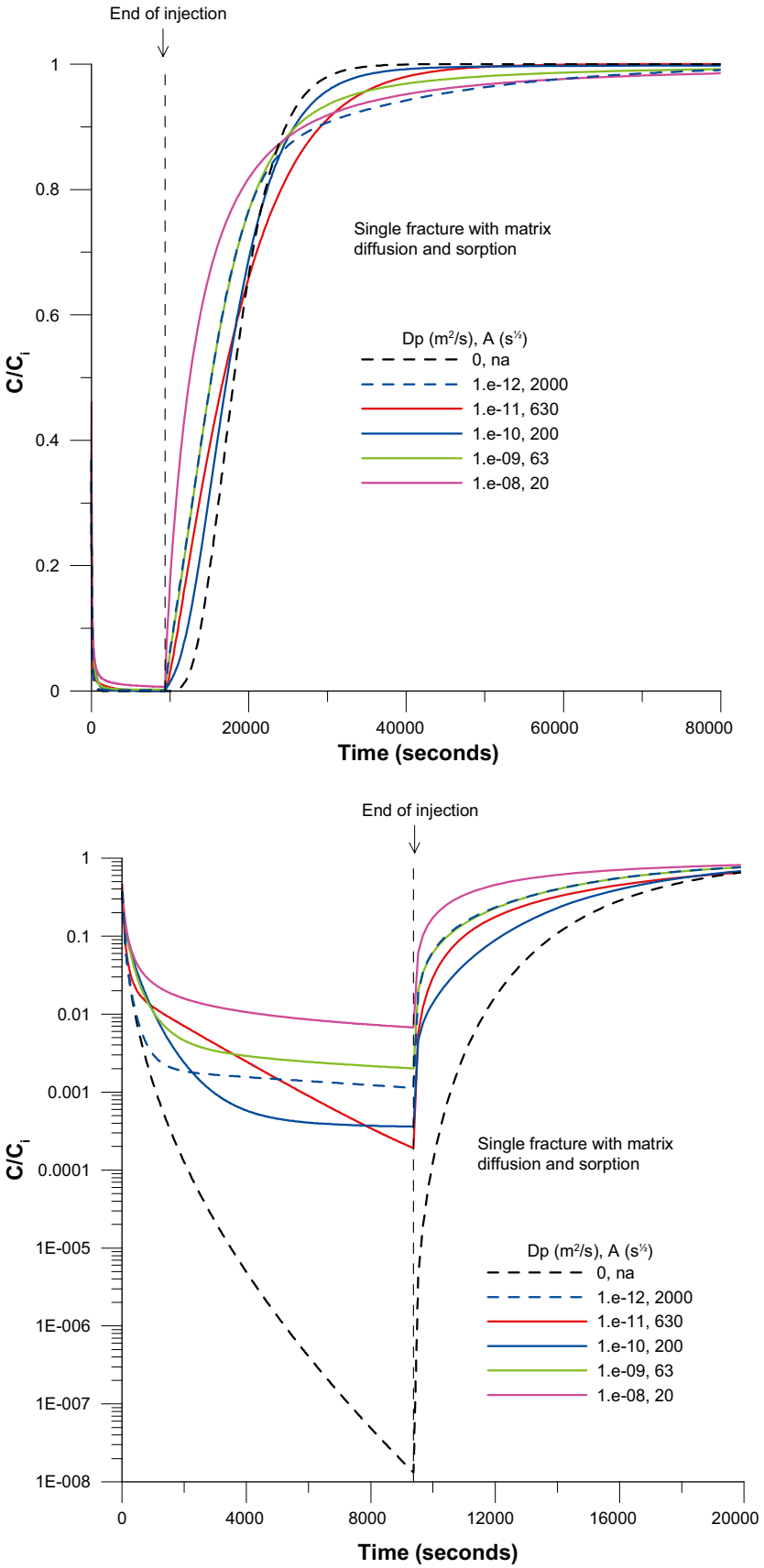

Figure 4-13. *Simulated tracer breakthrough in the SWIW borehole section in a single fracture with matrix diffusion and sorption in the matrix plotted in linear (top) and semilogarithmic (bottom) scale. The matrix porosity is set to 1 x 10^{-3} and the sorption coefficient to 1 x 10^{-3} m^3/kg.*

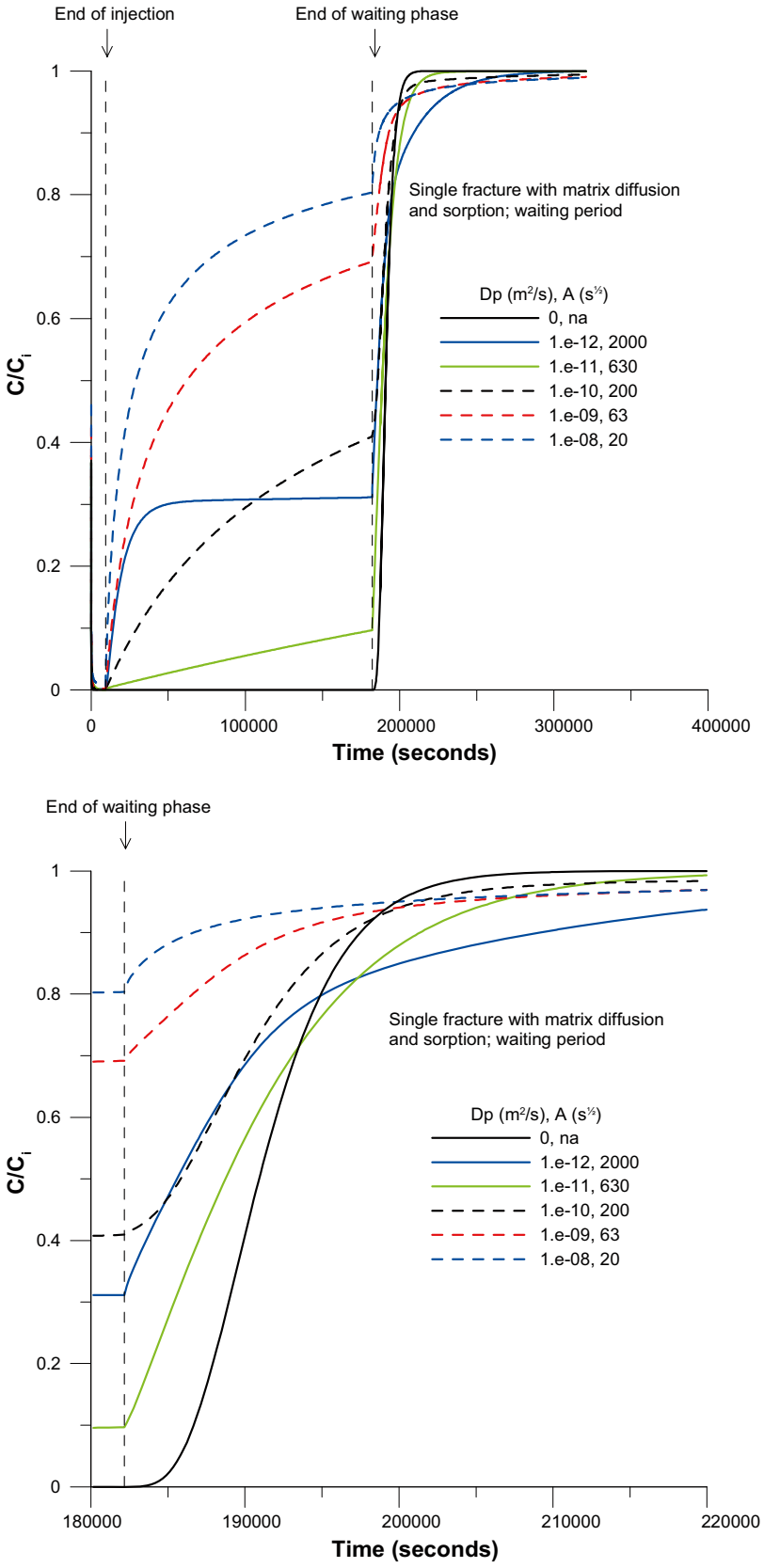

Figure 4-14. *Simulated breakthrough in the SWIW borehole section of sorbing tracers in a single fracture with matrix diffusion and a waiting period of 48 hour. The entire simulation sequence (top) is shown as well as a detailed plot of the recovery phase (bottom). The matrix porosity is set to 1 x 10^{-3} and the sorption coefficient to 1 x 10^{-3} m^3/kg.*

4.3.4 Single fracture with a high-porosity stagnant zone

This simulation example is somewhat similar to the matrix diffusion case, but instead of a relatively extensive low-porosity matrix there is a relatively small (0.4 mm) stagnant (with respect to flow) zone with a very high porosity (set to 1.0 in the simulations). In this case, "D_P" is actually the diffusion coefficient in the stagnant zone and, thus, one would expect the upper part of the D_p-range as more likely. The diffusion effects are in this case fairly visible even without a waiting period (Figure 4-15). For the higher diffusivity values (no values of A are given because the size of the stagnant zone is somewhat arbitrarily chosen), the effects are seemingly smaller because the tracers diffuses so fast out into the flowing fracture and more or less empties the stagnant zone. Instead, the largest effects occur at some intermediate diffusion value. It should be pointed out that the appearance of such effects depends largely on the assumed size and diffusion properties of the stagnant zone. The point to make here is that stagnant-zone storage with relatively fast transfer between the fracture and the stagnant zone give considerably different results than for a fracture with a low-porosity matrix.

The case with a waiting period (Figure 4-16) further illustrates the somewhat complex effects of diffusion into stagnant zones. In this case, the visible effects increase for decreasing diffusivity, i.e. decreasing rate of exchange between the stagnant zone and fracture. This happens because the stagnant zone is comprised of a limited volume that gets partially depleted, depending on the exchange rate, of solutes during the injection phase. For example, the simulated breakthrough curve for the lowest diffusivity value in Figure 4-16 attains the highest value, of the simulated curves shown, at the end of the waiting period because more tracer is left in the stagnant zone at the end of the tracer injection period.

4.3.5 Single fracture with matrix diffusion and a stagnant zone

The last simulation geometry example comprises a layered system with a single flowing fracture, a high-porosity stagnant zone and a low-porosity rock matrix. Not surprisingly, based on preceding example, this system is dominated by effects caused by the stagnant high-porosity zone, especially when no waiting period is employed. For the non-sorbing cases, results are similar to the results with a stagnant zone only and those cases are not shown here. Sorption in the matrix, on the other hand, may influence results in this simulation geometry. Figure 4-17 shows simulated breakthrough curves for sorbing tracers with a waiting period of 48 hours.

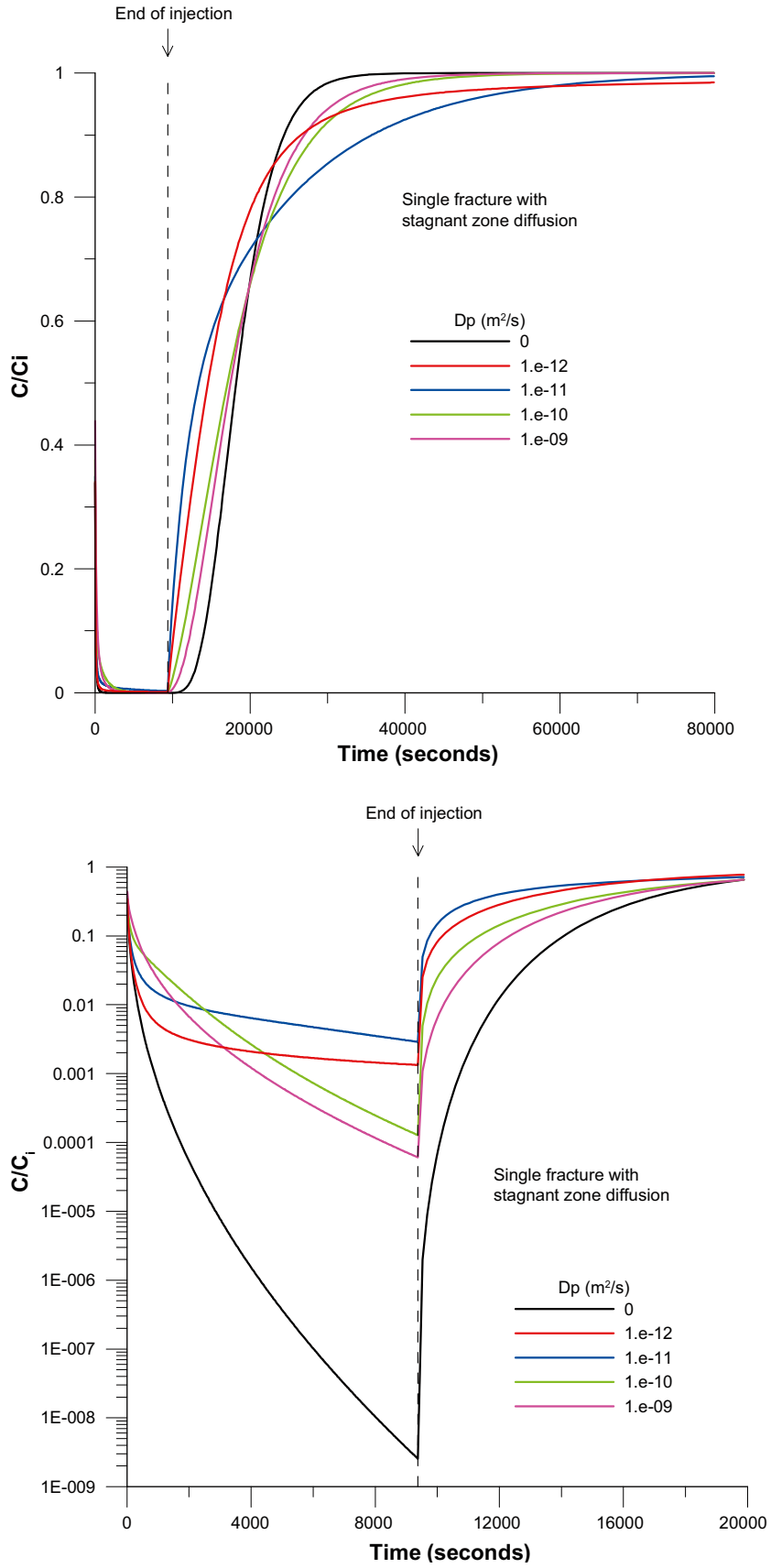

Figure 4-15. *Simulated breakthrough in the SWIW borehole section of non-sorbing tracers in a single fracture with a high-porosity stagnant zone plotted in linear (top) and semi-logarithmic (bottom) scale.*

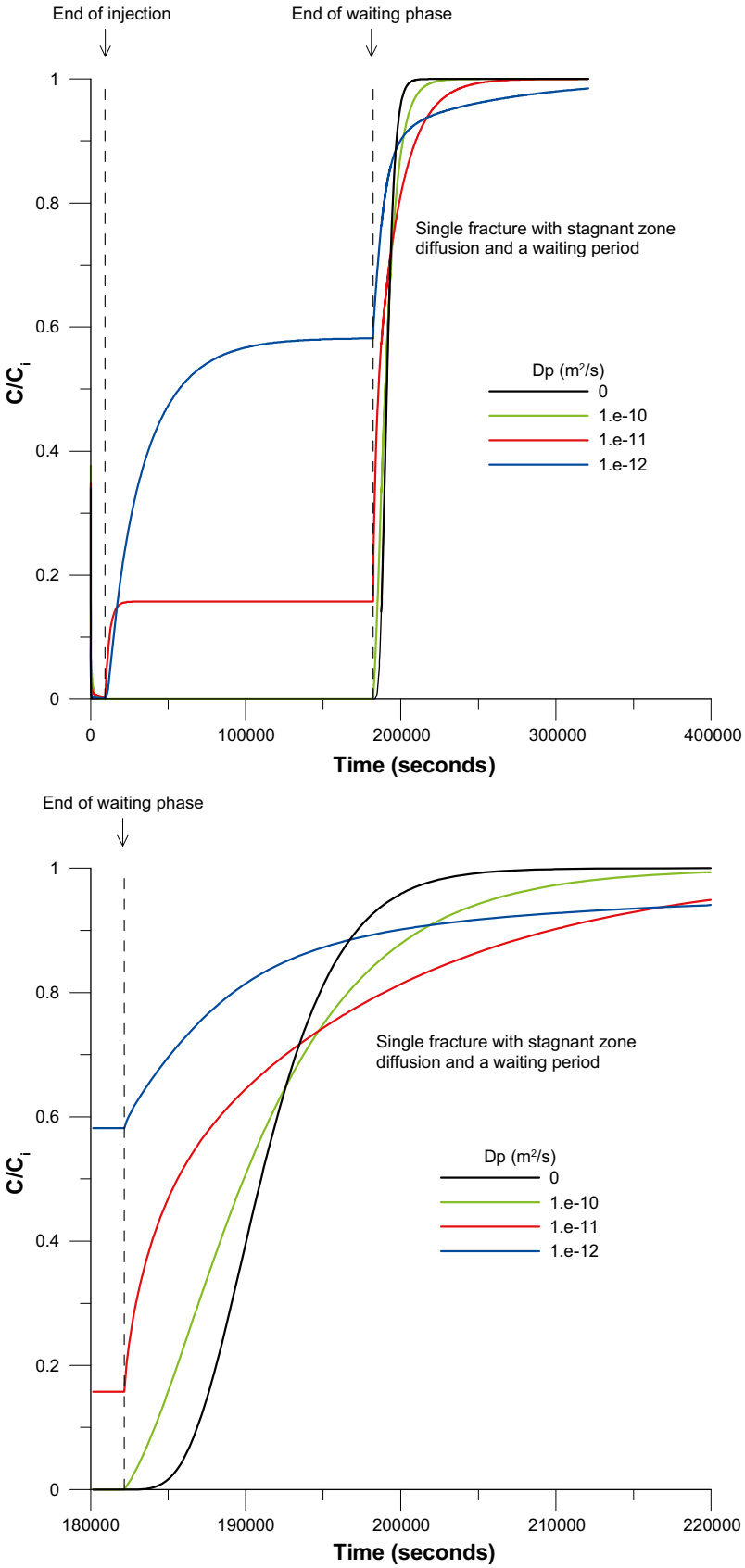

Figure 4-16. *Simulated breakthrough in the SWIW borehole section of non-sorbing tracers in a single fracture with a high-porosity stagnant zone and a waiting period of 48 hours. The entire simulation sequence (top) is shown as well as a detailed plot of the recovery phase (bottom).*

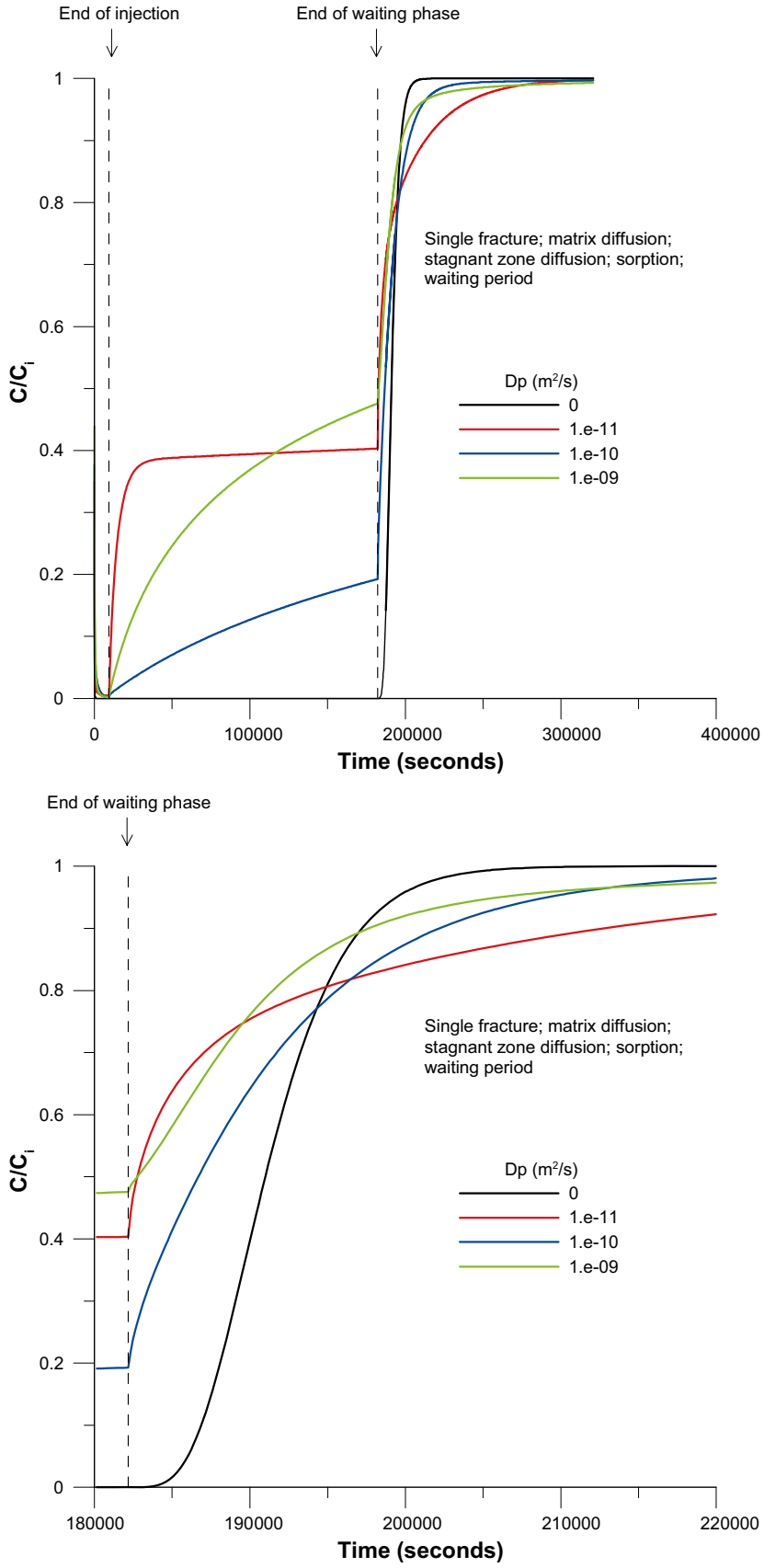

Figure 4-17. *Simulated tracer breakthrough in the SWIW borehole section in a single fracture with matrix diffusion, stagnant zone diffusion, sorption and a waiting period of 48 hours. The entire simulation sequence (top) is shown as well as a detailed plot of the recovery phase (bottom). The matrix porosity is set to 1 x 10^{-3} and the sorption coefficient to 1 x 10^{-3} m^3/kg.*

4.3.6 Comparison of tracer breakthrough in different simulation geometries

The preceding plots show simulated tracer breakthrough curves for ranges of diffusive effect in each hypothesized geometry separately, which is useful for understanding of the various processes and effects. One of the aims of the proposed experiment is to, if possible, discriminate between dominant transport processes/geometries and it is therefore useful to compare simulation geometries for a given set of model parameters.

In order to compare the effects of the various simulation geometries, this section presents several plots with a given (selected) diffusion rate. Figure 4-18 shows a comparison between simulation geometries for non-sorbing and sorbing tracers and without a waiting period. The selected case is for $D_p = 1 \times 10^{-9}$ m^2/s (i.e. $A = 3.16 \times 10^3$ s^{½}). For non-sorbing tracers, only relatively fast exchange with high-porosity stagnant zones give a visible effect compared with the case of no diffusion (i.e. flowing fracture only), as might be expected. The contribution of the low-porosity matrix is very small as the experimental time frame is very short.

For sorbing tracers, the comparison between simulation geometries gives larger differences between the cases with and without diffusion, respectively. The effect of sorption in the matrix may give a significant effect, regardless whether a layer of high-porosity stagnant zone is present or not. However, it may also be difficult discriminate between diffusive processes and equilibrium retardation in the fracture (in Figure 4-18 the black dashed line correspond to R=7 in Figure 4-8 for a single fracture). One might assume that it would be the end of the breakthrough curve that would be the best part for identifying diffusion processes.

A comparison of simulated breakthrough of non-sorbing tracers and sorbing tracers when a waiting period of 48 hours is employed (Figure 4-19) shows that, for non-sorbing tracers, effects of matrix diffusion in this case are somewhat more visible. This happens primarily at early times of the breakthrough curve, compared with the non-diffusive case, while at later times the matrix diffusion case becomes more similar to the non-diffusive.

For the sorbing tracers and a waiting period of 48 hours there is a relatively large difference between effects of matrix/stagnant zones and conservative transport in the flowing fracture. This happens because tracers are sorbed in the matrix and the matrix/fracture interface during the injection period.

The sorbing cases should be regarded as extreme with strong sorption, considerably more moderately sorbing tracers will be studied in the proposed SWIW test and results would likely fall some where in-between.

4.4 Different aspects on production of synthetic groundwater

4.4.1 Deionized water

Large quantities of deionized water may be obtained from CLAB containing for example, less than 3 ppb of Cl^-. The natural concentration of Cl^- in groundwater from Äspö (see Table 4-7) is about 2 million times higher than in the deionized water. In theory, it is possible to detect a mixing caused by diffusion in the range of one to a million which is very promising.

However, it should be pointed out that usage of deionized water will create salt gradients in the diffusion which will make the interpretation of the diffusion characteristics more uncertain. For example, the diffusion rate of non-sorbing anions will be affected by the diffusion rate of cations in order to obtain the electron neutrality. Hence, it would be preferable to manufacture a synthetic groundwater with the same ion strength as the natural groundwater, but with the main components exchanged for other elements.

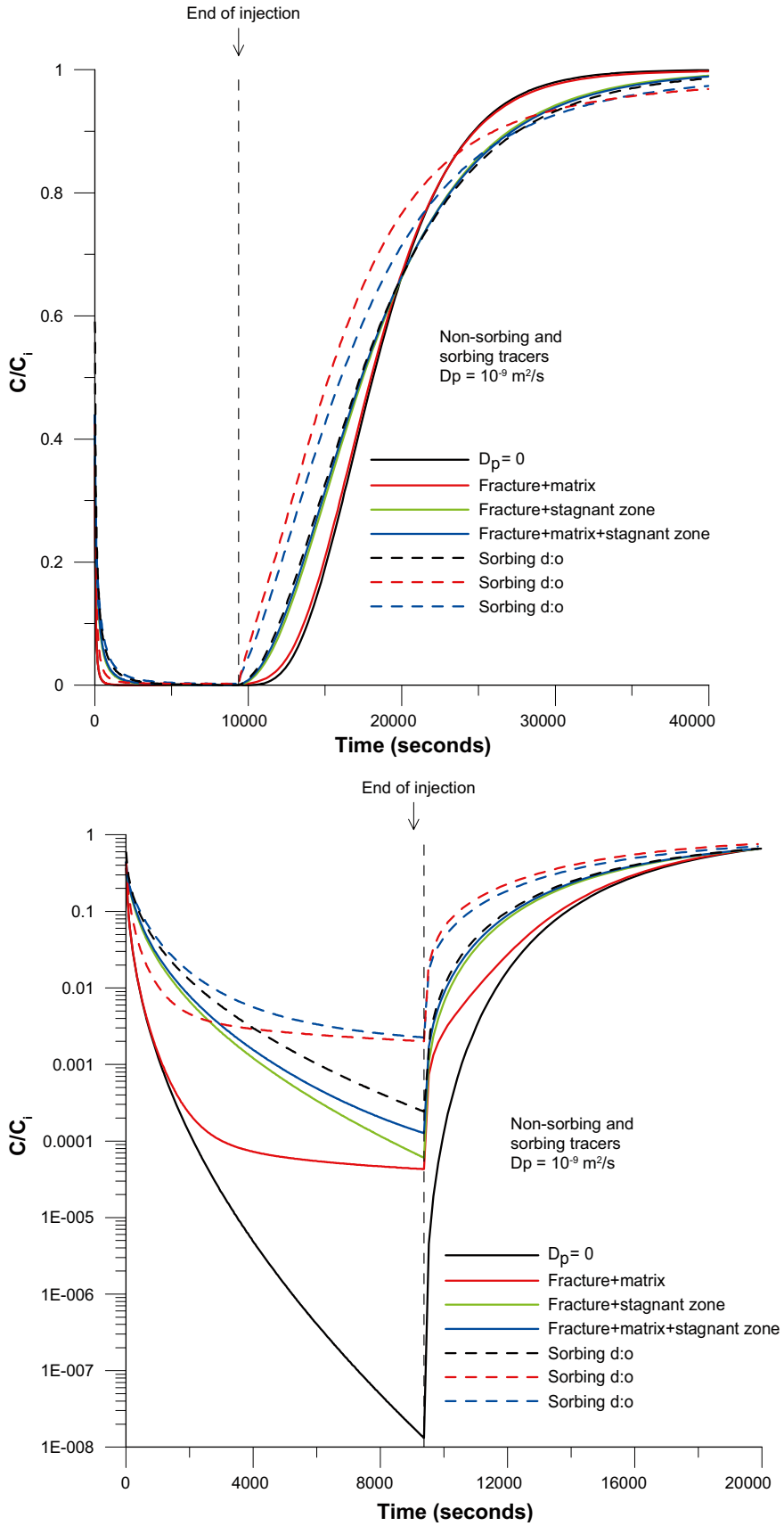

Figure 4-18. *Comparison of simulation geometries in the SWIW borehole section for non-sorbing and sorbing tracers plotted in linear (top) and semi-logarithmic (bottom) scale. The matrix porosity is set to 1 x 10^{-3} and the sorption coefficient to 1 x 10^{-3} m^3/kg.*

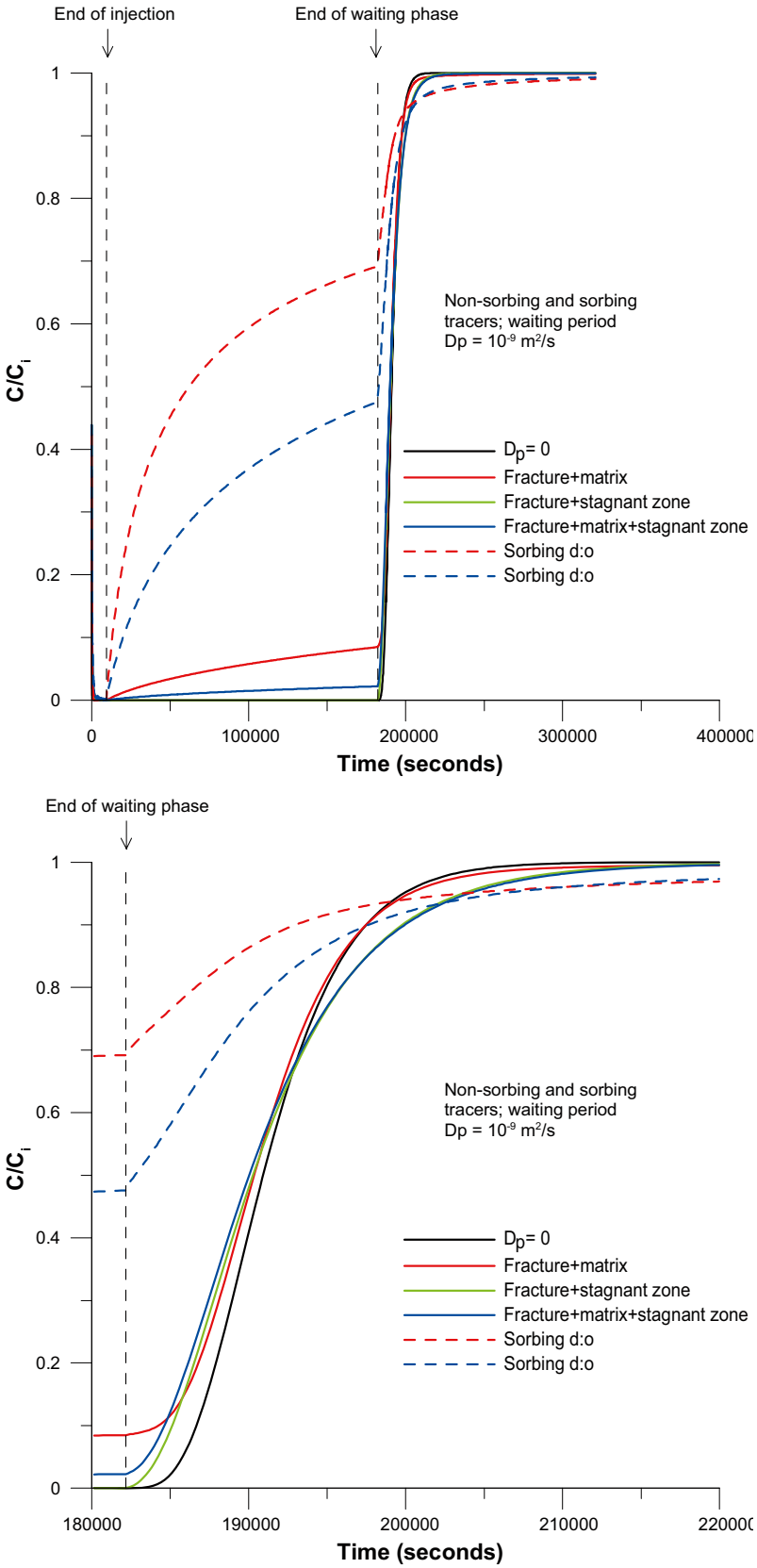

Figure 4-19. *Comparison of simulation geometries for non-sorbing and sorbing tracers and a waiting period of 48 hours in the SWIW borehole section. The entire simulation sequence (top) is shown as well as a detailed plot of the recovery phase (bottom). The matrix porosity is set to 1 x 10^{-3} and the sorption coefficient to 1 x 10^{-3} m^3/kg.*

4.4.2 Proposed composition of synthetic groundwater

A proposed composition for synthetic groundwater to use in this SWIW test is displayed in Table 4-7.

It is obvious that eventual diffusion from the matrix will cause a very small mass transport out into the synthetic groundwater in the fracture. For this reason, it is very important that it is possible to manufacture synthetic groundwater with very small contaminations of the studied components. Therefore, it is obvious that the salts used for the production contains very low contamination of Cl^-, Na^+ and Ca^{2+}. This is complicated by the fact that these components are very common contaminants in chemicals. It may therefore be necessary to purchase chemicals with very high purity to a potentially high cost.

A test of this type may involve large quantities of injected water, which means that large volumes of synthetic groundwater may have to be produced. For this reason and costs in the project, it is predicted that the highest grades of purity for the chemicals may have to be excluded from the production. An optimization regarding costs and purity will be necessary.

A proposal for main component chemicals in the synthetic groundwater is presented in Table 4-8. The cost for chemicals in this suggestion is about 70 SEK per litre and results in a contamination of about 10 times higher than in the deionized water. It will give a dynamic range (the concentration quotient of the natural and synthetic groundwater) between $3 \cdot 10^4$ and $1 \cdot 10^5$.

Table 4-7. Main components in natural groundwater from Äspö /Byegård et al. 1998/ and proposed replacements.

Component	C (ppm)	C (M)	Replaced with in the synthetic groundwater	C(ppm)
Cl^-	5,400	0.15	NO_3^-	9,300
Na^+	1,735	0.075	Li^+	520
Ca^{2+}	1,310	0.033	Mg^{2+}	794
SO_4^{2-}	305	0.003	(SO_4^{2-})	305

Table 4-8. Proposed chemicals for the synthetic groundwater.

Chemical	Purity	g/litre of water	Cost [a]	Contamination in chemical (ppm)			Contamination in synth. groundwater (ppb)			Cost ground water (SEK per litre)
				Cl^-	Na^+	Ca^{2+}	Cl^-	Na^+	Ca^{2+}	
Li_2CO_3	≥ 99.99%	2.79	1,870 SEK per 100 g	10	10	5	28	28	14	52
HNO_3	≥ 69% [1]	17.75	3,500 SEK per 4,200 g	0.3	0.01	0.01	5	0.2	0.2	15
Mg	99.98%	0.79	1,200 SEK per 1,000 g	5	30	7	4	24	6	4
Li_2SO_4	≥ 99.0%	0.20	874 SEK per 500 g	20	50	10	4	10	2	0.4
Total							41	62	22	71
Natural groundwater							5.4E+6	1.7E+6	1.3E+6	
Dynamic range							1.3E+5	2.8E+4	6.3E+4	

[a] From Sigma-Aldrich 2007

4.5 Different aspects on the application of radon measurements

As can be seen in the theories for the diffusion calculation (Section 4.3.2), modelling of the breakthrough curve will only give a value of the A-parameter which in itself is a lumped parameter including the fracture aperture, the porosity, the diffusivity and (in the case of a sorbing tracer) the sorption coefficient. It would thus be convenient if an independent measurement of especially the fracture aperture could be obtained and used in the evaluation.

In /Byegård et al. 2002/ different aspects are presented for the application of radon measurements for estimation of the fracture aperture. In its simplest model approach (the surface production model) a constant flux of radon atoms diffuses from the matrix into the fracture. A steady-state is then obtained when the rate of radon atoms diffusing into the fracture surface equals the decay rate in the water in the fracture groundwater. One can therefore easily realise that for a given flux ($n \cdot m^{-2} \cdot s^{-1}$, n is number of radon atoms) of radon atoms, the activity concentration ($n \cdot m^{-3} \cdot s^{-1}$) is inversely proportional to the fracture aperture (m).The radon flux can thus be determined in laboratory experiments in which the radon concentration is measured in a given volume of water which has been in contact with a given rock surface area for times long enough to ensure that a steady state will be obtained (typically 1 month). Results from such experiments are presented in /Byegård et al. 2002/, in which fluxes in the range of 70–200 $n \cdot m^{-2} \cdot s^{-1}$are presented for Fine grained granite, 6–16 $n \cdot m^{-2} \cdot s^{-1}$ for Äspö diorite and $< 11\ n \cdot m^{-2} \cdot s^{-1}$ for mylonite sampled closest to the Feature A fracture used for tracer experiments in the TRUE-1 project /Winberg et al. 2000/. Application of the $< 11\ n \cdot m^{-2} \cdot s^{-1}$ detection limit with the radon concentration measured in the Feature A (400,000 $n \cdot m^{-3} \cdot s^{-1}$) would correspond to a half aperture of < 0.03 mm.

/Neretnieks 2002/ applies a more sophisticated method in which the radon flux is interpreted from a matrix diffusion concept. This results in a gradient from the fracture towards the inner parts of the rock matrix and one will thus also have to consider backdiffusion from the fracture into the matrix. Contrary to the simple radon flux concept described above, the net number of radon atom flux into the fracture will therefore not be independent of the fracture aperture. Since laboratory experiments of the radon flux is necessary to perform using a much higher water/rock surface area ratio than in a natural fracture, the results of the laboratory experiment can thus not be used as straight-forwardly as in the simple concept above.

For a matrix diffusion interpretation of the fracture aperture using the radon concentration in the groundwater, one therefore has to involve the matrix diffusion parameters, i.e. (provided that radon can be considered as a non-sorbing tracer) the porosity and the pore diffusivity. One also of course has to know the source term, i.e. the number of radon atoms produced in the rock matrix per time unit. This term of course corresponds to the concentration of Ra-226 in the rock matrix and should therefore be possible to obtain an accurate independent measure of. However, /Neretnieks 2002/ also in his concept distinguishes between radon atoms that after its production (i.e. the Ra decay) reaches the pore water (mobile) and the radon atoms that will be trapped in the crystal lattice (non-mobile). The term "release factor" (η) is therefore introduced to compensate for the non-mobile radon atoms, the total number of Ra-226 atoms multiplied with release factor is thus the source term for the mobile Rn-222 production. Nevertheless, the net outcome is that three different parameters, i.e. porosity, pore diffusivity and the release factor, have to be determined from the data obtained in the laboratory experiment if the *in situ* radon concentrations should be possible to use for the determination of the fracture aperture.

Some preliminary comparative calculations made by /Neretnieks 2002/ indicate that the smaller the fracture aperture gets, the larger deviation is obtained between a simple surface production model and the diffusion model.

One can therefore identify and summarize the general limitation of the concept of using *in situ* radon concentrations in combination with radon flux laboratory experiment for estimation of the fracture aperture:

- The surface production model offers a straight-forward way of applying laboratory results and *in situ* radon concentrations to calculate the fracture aperture. However, according to a matrix diffusion concept, this model is found to give an overestimation of the radon flux and therefore also an overestimation of the fracture aperture.
- For the matrix diffusion concept, one needs the numerical values from three independent parameters (porosity, pore diffusivity and the release factor) to be able to apply the *in situ* radon concentrations to calculate the fracture aperture. Since methods for independent measurements of the porosity and the pore diffusivity exist, it is theoretically possible that the measured radon concentration in the laboratory experiment should correspond directly to the release factor. However, it is likely that the involvement and combinations of these many parameters will result in a considerable uncertainty associated with the calculated fracture aperture value.
- A problem involved for both concepts is to what degree a limited number of rock samples used for the laboratory experiments can give a representation of the properties of the entire fracture studied in the *in situ* experiment. It is easy to realize that a realistic case may be that one only has rock material from the intersection between the borehole and the fracture, which definitely is questionable from a representativity point of view. One can also foresee that all supporting measurements, i.e. the Ra-226 analyses, the porosity and diffusivity measurements, are necessary to be done using the same intersection rock sample which may give different practical problems.

An advantage with addressing this radon concept in the proposed SWIW experiment with synthetic groundwater is that it will thus be possible to obtain diffusion characteristics from two sets of non-sorbing tracers, e.g. chloride that due to the diffusion will be depleted from the rock matrix and radon that besides the depletion due to the diffusion will be influenced by in-growth due to the decay of Ra-226. A simultaneous evaluation of these two characteristically different breakthrough curves for non-sorbing tracers together with the measured natural steady-state concentration of Rn-222 may increase the possibility of identifying unique values of the parameters, perhaps even without having to address the results of the laboratory experiments on samples which representativeness could be questioned. Further scoping calculations addressing the radon concepts will be necessary to evaluate these possibilities.

A crucial point using Rn-222 as tracer is of course the contact time. Applying short experimental times give low time for in-growth of Rn-222 which may constitute a problem. On the other hand, long contact times (typically over 3 half–li.e. i.e. approximately 10 days) may result in a withdrawal water that has come very close to the natural steady state conditions. One should be aware of that a detection limit of Rn-222 in groundwater of 0.03 Bq per liter has been reported and that a Rn-222 concentration in the range of 75–320 Bq per liter has been observed for groundwater sampled in structure #19 in TRUE Block Scale. That means that dynamic ranges in the order of $2.5 \cdot 10^3$–$11 \cdot 10^3$ are obtained which should make it possible to study the in-diffusion/in-growth of Rn-222 using comparatively short contact times. Which contact time that offers the best sensitivity for obtaining diffusion characteristics can, however, not be predicted without making more elaborate scoping calculations. A general estimate is however that after 3 half–li.e. ~12 days, the in-growth should be close to 90% of the radioactive equilibrium and one may assume that the Rn-222 concentration should be very close to the steady-state conditions. One may therefore roughly give 12 days as the maximum contact time in a SWIW experiment if one aims to obtain useful information of the Rn-222 tracer.

The simulations presented in this report use a maximum contact time approximately 2 days for the case of applying a waiting time and 4 hours for the case without waiting time. One may foresee that at least the latter case may be chosen a little short for optimum use of the Rn-222 tracer.

Some practical problem can be identified using Rn-222 as tracer. During the withdrawal phase, the last part of the "travel" of the groundwater will be in the borehole section and finally through the plastic tubing of the borehole equipment. During these steps, the in-diffusion of Rn-222 will be significantly lower due to the much lower rock surface area versus groundwater volume ratio. However, the radioactive decay will of course proceed which will give radon concentrations in the sampling in the tunnel that is not fully representative for the fracture groundwater. It is obvious that a minimization of the duration time in the borehole section is favorable.

In the TRUE Block Scale continuation experiment /Andersson et al. 2004/ a borehole volume of approximately 8 dm^3 was applied for the borehole section KI0025F02 in structure #19. Applying the flow rate proposed in the scoping calculations in this report (14.4 dm^3/h) one obtains a duration time of 0.5 h in the bore section. This corresponds to a 0.4% decrease of the Rn-222 activity which probably is within the uncertainty of the Rn-222 measurement. However, different interactions and losses of radon (as well as other dissolved gasses) with nylon tubing has been observed (e.g. /Andersson et al. 2000/, /Holmqvist et al. 2002/) which is likely to complicate the experiment, especially since the mechanisms of these interactions are poorly known. The conclusions of /Holmqvist et al. 2002/ and /Andersson et al. 2002/ is that metal equipment in the experiment can solve these problems.

4.6 Estimated costs

The following cost estimation of the performance of SWIW tests with synthetic groundwater is rough and should only be considered as a guideline. A requirement for this estimation is that the site is well characterized (as for example TRUE-BS) and prepared for use. The equipment necessary for the experiments is similar to the equipment used in earlier experiments at TRUE-BS and TRUE-1 so it is assumed to be available and not included in this estimate.

The estimation in Table 4-9 includes the following elements:

- Dilution test under natural conditions.
- SWIW-pretest with non-sorbing tracers (without synthetic groundwater).
- SWIW-test with synthetic groundwater without waiting phase.
- SWIW-test with synthetic groundwater with waiting phase.
- Production of synthetic groundwater.
- Evaluation, modelling and reporting of the tests.

If multiple boreholes are available, crosswise stressed dilution and interference test could be performed and evaluated as well as additional sampling and analysis of water from observation holes during the SWIW tests. The estimated extra costs for these options are listed in Table 4-10 and 4-11. However, note that these costs are based on a couple of extra boreholes in the area and less extensive sampling in the observation holes than in the SWIW borehole section. If more boreholes will be used the cost will probably increase.

As noted above, the cost estimation assumes that a test site is available and ready to be used. It is not included in the feasibility study to estimate such costs but a rough estimate is that a new site will cost between 2,000 and 3,000 kSEK depending on the number of drilled boreholes, instrumentation and investigations used in the characterization of the site. However, the projects *Oxygen consumption and redox changes in a fractured zone – SWIW test* and *Multiple well experiment* will probably use the same site as SWIW test with synthetic groundwater whereas this cost could be shared by the projects.

Table 4-9. Estimated costs for performance and evaluation of SWIW tests with synthetic groundwater.

Field performance	Costs kSEK
Project management and planning	80
Pretest, dilution test	60
Pretest, SWIW	150
SWIW, without waiting period	150
SWIW, with waiting period	150
Production of synthetic groundwater	100
Analysis	260
Sum Field performance	950

Evaluation	Costs kSEK
Project management and planning	30
Modelling	160
Evaluation, conclusions	100
Reporting	260
Sum Evaluation	550

Table 4-10. Additional costs for crosswise stressed dilution and interference test.

Crosswise stressed dilution and interference test	Costs kSEK
Field performance	80
Analysis	60
Modelling, evaluation, reporting	90
Sum	230

Table 4-11. Additional costs for sampling in observation holes during SWIW tests.

Additional sampling in observtion holes during SWIW	Costs kSEK
Analysis	90
Modelling, evaluation, reporting	150
Sum	240

5 Discussion and conclusions

5.1 Summary and recommendations based on scoping simulation results

The scoping simulations presented above show, despite that the studied examples are comprised of simple systems and do not cover all possible combinations of transport domain attributes, that a wide range of tracer behaviour may be expected depending on the relative influences of stagnant zones, rock matrix and sorption in the fracture. Expected results are complex because the induced flow during the injection in the flowing fracture carries tracer away that may have been picked up from stagnant zones and/or the matrix. Tracers with different diffusion and sorption properties have the potential to show differences between different transport geometries. It will likely be important to use a combination of as many tracers with different diffusion and sorption properties as possible.

The proposed SWIW experiment presents a possibility to use a relatively large number of tracers with different properties which provides better opportunities to use combinations of tracers to constrain interpretation of experimental results. It should also have the potential to provide valuable opportunities to study a number of interesting aspects regarding SWIW experiments in general. For example, it should be possible to study possible differences depending on which rock volume is tested, i.e. comparing breakthrough from injected tracers with tracer already present in the formation.

One might argue that there are no obvious unique effects for a single tracer, which would also be the case for any tracer test. Instead, one must rely on combinations of tracers with different properties for interpretation. Unlike the scoping simulation results presented, it will not be possible in an actual experiment to have a completely non-diffusive tracer. Interpretations of diffusion effects in matrix and/or stagnant zones during tracer tests are typically made by fitting alternative models to experimental data. An even better possibility to study diffusion effects would be to have more than one non-sorbing tracer with different diffusion coefficients. In the proposed experiment, Uranine and chloride are planned to be used as non-sorbing tracers and their relative diffusivity (i.e. in water) may possibly be used to further constrain interpretation of diffusion effect; the D_w is 2E–9 m^2/s for chloride /Li and Gregory 1974/ and 0.5E–9 m^2/s for Uranine (estimation by /Skagius and Neretnieks 1986/). However, a drawback is that Uranine will be used as an artificially introduced tracer which breakthrough characteristics will be different from the naturally abundant chloride tracer. Consequently, it is preferred if naturally abundant non-sorbing tracer with diffusivities different from chloride could be used. Potential candidates are He dissolved in the groundwater (D_w=8E–9 m^2/s CRC Handbook) and SO_4^{2-} (D_w=1E–9 m^2/s / Li and Gregory, 1974/) which thus would offer a range of diffusivities by a factor of 6. These two compounds have been found in significant concentrations in the Äspö groundwater. He have e.g. been found in the range of 5–15 ml/l in the investigation of the boreholes KA3386A02–KA3386A06 /SICADA/ and SO_4^{2-} was measured in concentrations of ~300 ppm /Byegård et al.1998/. Regarding the general experiences of natural concentrations, detection limits and possibilities to prepare synthetic groundwater with absence of these tracers, it can be foreseen that they should be usable as tracers in the proposed type of experiment. However, some drawbacks can be identified for the use of these tracers:

- Diffusive losses of He due to interaction with plastic tubing has been reported /Holmqvist et al. 2002/ which is likely to complicate the use of this tracer. Use of He as a tracer would therefore need a careful choice of the borehole instrumentation material, e.g. use of metal tubing. Furthermore, the sampling and measurements are complicated by the risk of diffusive losses. Masspectrometric online measurements of He has been used in tracer experiments in the ÄHRL before /Holmqvist et al. 2002 and Andersson et al. 2002/; alternatively, sampling in e.g. pressurized stainless steel vessels may be applied to avoid diffusion losses from sampling to laboratory measurement.

- There are to our knowledge no results reported for using SO_4^{2-} (sulphate) as groundwater tracer. Due to its chemical properties, one may however assume that it should behave in a non-sorbing way. However, a problem could be to find a suitable analogous ion to replace SO_4^{2-} in the synthetic groundwater to maintain the ionic strength properties (cf. section 3.4). A possible candidate would be the chemical analogue SeO_4^{2-} which D_w has been reported to very close to SO_4^{2-} /Li and Gregory, 1974/. Some preliminary investigations of the possiblities of adding SeO_4^{2-} instead of SO_4^{2-} to the synthetic groundwater mixture are summarized in Appendix A. Compared to the original proposal (Table 4-8) it is obvious that particularly Na^+ impurities in the selenic acid will raise the concentration of that tracer in the synthetic groundwater. Chloride and sulphate impurities are not reported by the manufacturer so a conservative estimate is done which results in that the impurities from the selenic acid will be the major part of the impurities for these tracers. This would result in a decrease of the dynamic range for chloride from 1.3E+5 to 3E+4. This decrease may be crucial and may mask the possibilities of detecting a very low matrix diffusion input of chloride and one should therefore make careful considerations before including this tracer in the experiment concept.

In the proposed experiment, it is likely that only fast effects of diffusion of non-sorbing tracers would be visible during an experiment without a waiting period. Thus, this might be a way to identify high-porosity stagnant zone effects. In an experiment with a waiting period, matrix effects may be visible but possibly also to some extent obscured by stagnant zone effects. It should be reasonable to argue that repeated experiments, with and without waiting periods, respectively, would improve the possibilities to discriminate between those processes. The same tracers would then be studied and compared in both of the experiments. Different waiting times may reveal differences between fast and slow diffusion effects. No waiting time may be expected to give no visible effects of matrix diffusion, but diffusion effects may be visible if a high-porosity stagnant zone is present.

Breakthrough of sorbing tracers would be expected to be different from non-sorbing tracers regardless of transport geometry. Discriminating between sorption in the matrix and simple fracture sorption may be best accomplished when a waiting period is employed. However, in the case of a combination of stagnant zone/matrix it still may be difficult to discriminate between whether stagnant zone or matrix diffusion dominates. Also in this case it would seem interesting to compare results from repeated experiments, with and without waiting period, respectively.

A problem associated with use of sorbing tracers which can be regarded in the scoping calculation is that a comparatively low difference between the non-sorbing and sorbing tracers can be seen in the breakthrough curves. The sorption coefficient used (K_d=1E–3 m^3/kg) is furthermore much larger than what normally has been reported for the tracers proposed as sorbing tracers in the experiment (i.e. Na^+ and Ca 2^+) in saline groundwater environment. One can therefore identify a need of including a stronger sorbing tracer to the experiment. The only additional cation tracer that can be identified to be present in the natural concentrations enough to allow use in this type of experiment is K^+ which in the work of /Byegård et al. 1995/ was identified to be 5–10 times more strongly sorbing than Ca^{2+}. In Appendix A, an extended tracer proposal is given in which the content of K^+ in the synthetic groundwater is replaced with the analogous element Rb^+. Due to the comparatively low concentrations of K^+ in the groundwater combined with impurities of K^+ mainly in the $LiCO_3$, a rather low dynamic range is obtained for this tracer, i.e. ~300. The addition of $RbNO_3$ is not causing any predominant increase of the other tracers aimed to be studied, so from this perspective there are no restrictions identified in the use to include K^+ in the study.

When comparing the Kd in Appendix A, one should be aware of the general uncertainty associated with them, e.g. depending on contact time, particle size, water composition and evaluation concept /Byegård et al. 1998/. An additional complication concerning the sorbing tracers is that a different water composition is used during the injection process which is likely to change the adsorption characteristics of the tracers. For example, replacing of Ca^{2+} to Mg^{2+} involves addition of a major competing cation (Mg^{2+}) which, using cation exchange models, has been

indicated /Byegård et al. 1995/ to be a factor of ~10 more selective for adsorption compared to the natural major competing cation (Ca^{2+}). A general decrease of the adsorption of the other tracer is therefore likely to occur.

To make an address of these varying adsorption characteristics, one would probably have to do at least batch sorption experiment with using both the introduced synthetic water composition and the natural water composition. Nevertheless, the most interesting interactions of these experiments will take place in the gradient between these two extremes, which thus also would be favourable to address with batch sorption experiment. However, it is likely that this type of an elaborate addressing of the varying sorption coefficient must be considered as being beyond realistic objective of this investigation. The sorbing tracers should maybe be considered as included only for demonstrative purposes in which a numerical uncertainty/variation of the sorption coefficients within one order of magnitude is of less importance. What should be considered as more important is the behaviour of the different sorbing tracers in comparison to each other; the relative level of sorption $Na^{+} < Ca^{2+} < K^{+}$ must be considered as robust which will provide important qualitative information of the sorption interaction.

When employed, the waiting period itself may probably not be used for sampling because it is probably of higher priority not to hydraulically disturb the system during the waiting period. However, differences in tracers and transport geometries sometimes strongly affect the simulated results at the end of the waiting period and it might be of particular interest to obtain representative samples as early as possible during the recovery period. In fact, it may be possible that high initial concentrations at the beginning of the pumping phase following a waiting phase can be considered to be an indicator of diffusive exchange with stagnant zones. Back-diffusion of tracer into the borehole may occur during the waiting period; however, such processes have not been simulated herein.

Any observations that is possible to obtain of tracer breakthrough in an additional borehole at a moderate distance away from the SWIW section should be very valuable, which may be said about SWIW experiments in general. In particular, observations of sorbing tracers in a distant borehole give a more unambiguous effect of retardation effects.

The possibility to compare tracer breakthrough in two ways, i.e. in injected water and the "reverse" breakthrough from the formation water is likely to be very valuable from a method point-of-view, with respect to SWIW experiments. Results from SWIW experiments currently performed within the site investigation programmes appears to indicate that diffusive processes (from matrix and or stagnant zones) have an influence on experimental results. The herein proposed experiment will use a larger number of tracers, and it should be possible to obtain further indications of what type of transport processes influence SWIW tests.

Comparison of Uranine and chloride breakthrough may give an indication of differences depending on which rock volume the tracer experiences. This may provide additional valuable supporting information for interpretation of SWIW tests performed within the site investigations.

If a waiting period is applied, it is very important that the surrounding ambient flow conditions do not cause significant amount of tracer to be lost during the waiting period. This is of particular concern if the experiment is carried out in the vicinity of a tunnel or near other underground structures that may act as hydraulic sinks.

Sampling (pumping) for a long time may collect more distant ambient water with different chemical properties, this may be a confusing factor for interpretation of the experiment, especially for the tail of the experimental breakthrough curve.

The scoping simulations presented here are for only a limited combination of geometries. Further, the assignment of transport properties is very simplified. For example, the same diffusivity value is used for all simulated parts, i.e. effects of tortuosity and constrictivity are not fully accounted for. Another limitation is that, for the more complex geometries, sorption in the flowing fracture or in the high-porosity stagnant zone is neglected.

5.2 Summary and recommendations regarded site selection

As indicated both by previous experiences and the simulations carried out in this study there are several characteristics that have to be considered for a site selection for a SWIW test. Some of the features are preferable in order to obtain a high recovery and others are wanted to facilitate the evaluation of the SWIW test.

The preferable features of a site for a SWIW test is a well characterized site with a low hydraulic gradient without any highly conductive hydraulic features in the vicinity. If the hydraulic gradient in the structure is too large it could pose a problem for the recovery since the tracers could travel away from the test section. The tracers that end up in a highly conductive feature could be impossible to pump back to the test section resulting in a low recovery. This type of highly conductivity feature includes, of course, the tunnel itself. Hence, the target structure should not be too close to the tunnel. However, it should not be too far away either since the consequence is large volumes in hoses etc. It is difficult to give any exact figures about the preferable distance from the tunnel to the target structure. However, in TRUE-BS several successful tracer tests were performed in #19 which is approximately 150 m from the tunnel so this distance should be acceptable. The TRUE-1 site was only c 15 m from the structure to the tunnel which may have contributed to the relatively low recovery. Hence, a distance of c 50–150 m from the tunnel to the structure would be preferable. However, this depends of course on other elements such as hydraulic transmissivity and gradient. It is also desirable that the target structure is rather simple which facilitates the evaluation of the test. If there are other boreholes in the vicinity that intercept the structure it could be an advantage for the evaluation and understanding of the test since sampling of these boreholes could provide breakthrough curves at some points in the fracture. The preferable characteristics of a site for SWIW with synthetic groundwater may be summarized in the following list:

- a well characterized site,
- a low hydraulic gradient in the target structure,
- no highly conductive hydraulic features in the vicinity, including the tunnel itself,
- the target structure should not be too far away or too close to the tunnel wall,
- intercepting observation holes in the target structure,
- a simple geometry of the target structure.

The two projects *Oxygen consumption and redox changes in a fractured zone – SWIW test* and *Multiple well experiment* will probably prefer the same characteristics of the site. Hence, there will be significant coordination effects between the three projects in choosing and preparation of a test site. The other two projects are currently in the planning stadium and will probably be performed after SWIW with synthetic groundwater.

As shown in this report, several tracer tests in between sections in TRUE-BS have resulted in a high recovery. However, this fact in itself does not implicate that a high recovery is given for SWIW tests since the configuration of the previous tests and the SWIW test are different. However, a high recovery for a tracer tests in between two sections in combination with a rather low hydraulic gradient and no major hydraulic features in the vicinity are considered to be a strong indication of a site suitable for SWIW tests. Hence, target structure #19 in TRUE-BS may be used for SWIW tests with synthetic groundwater. The section KI0025F03:R3 has previously been used successfully in earlier tracer tests and should probably also be suitable for these SWIW tests. Also target structure #20 could be used but since one of the boreholes has a shortcut in the packer system this structure is considered as less appropriate for the tests. Another advantage of using the TRUE-BS is that the results of the SWIW tests may be compared to earlier performed tracer tests at the same site. However, since only pressure data is available to judge if the TRUE-BS is unaltered hydrologically, this should be verified by dilution tests and some crosswise interference tests before performance of SWIW tests at the site.

As pointed out above, the TRUE-BS site would be suitable for these tests if the site characteristics would be unaltered since the late fall of 2006. However, since that time the project *"Fintätning av tunnel på stort djup"* has started close to the site. It should be pointed out that the plans for *"Fintätning av tunnel på stort djup"* were unknown by the authors at the beginning of this study. In short, this project will result in a new tunnel close to TRUE-BS. During the construction time of this tunnel, the hydraulic conditions in TRUE-BS will probably vary over time so it is not a good idea to perform SWIW tests there during this time. After the completion of the tunnel it may be possible to perform the SWIW tests. However, there exists a great risk that the tunnel alters the hydraulic conditions of TRUE-BS so that it will be impossible to perform a successful SWIW test. Even if the hydraulic alteration of the site is minor so that it is possible to perform the SWIW tests, there will exist uncertainties about comparison with earlier performed tracer tests at the site. Another factor is the time aspect since the new tunnel, according to the time table, will be completed during the early spring of 2009. The consequence is that the earliest time we will know whether TRUE-BS is suitable or not is 2009. Considering SKB:s general time table and that two other projects will follow SWIW with synthetic groundwater this significant delay of the time table may be problematic.

The alternative to TRUE-BS is to find another site in the Äspö tunnel. No other sites than TRUE-BS was considered in this study so no alternative sites will be suggested here. However, it is suggested that both existing sites and new sites should be considered in a future site selection. If a new or less characterized site is chosen for the performance of these tests, additional boreholes and hydrological and geological investigations will be necessary prior to the experiments. This will of course lead to additional costs in the project. However, since two other projects probably will share the same site and infrastructure, the costs will also be shared.

5.3 Proposed tests and pre-tests

Before any SWIW tests are performed within the project, the chosen site should be well characterized with respect to hydrogeology, geology and mineralogy. Whether TRUE-BS or some other site will be used for SWIW with synthetic groundwater the following tests are proposed:

1. Dilution test under natural conditions.
2. Crosswise stressed dilution and interference test (if multiple boreholes are available).
3. SWIW-test with non-sorbing tracers (without synthetic groundwater).
4. SWIW-test with synthetic groundwater without waiting phase.
5. SWIW-test with synthetic groundwater with waiting phase.

5.4 Conclusions

The conclusions of this feasibility study may be summarized as follows:

- SWIW tests with synthetic groundwater have the potential to provide new opportunities to discriminate between fast and slow diffusion processes (i.e. diffusion from stagnant zones and rock matrix) by applying different waiting periods in the experiments.
- SWIW tests with synthetic groundwater are likely to give valuable information for interpretation of SWIW tests performed within SKB:s site investigation programme.
- Observations of tracer breakthrough in additional boreholes at a moderate distance away from the SWIW section should be very valuable for interpretation of the experiment in particular and for SWIW tests in general.
- It is possible to produce synthetic groundwater with an altered composition of a sufficient amount and purity to perform SWIW tests with synthetic groundwater.

- Usage of radon measurements in the experiments may provide additional information due to different diffusion characteristics from the rock matrix than other species. However, if radon measurements will be used in the experiments, further scoping calculations regarding radon would be preferable.
- TRUE Block Scale may be suitable as a test site for SWIW tests with synthetic groundwater. However, presently a new tunnel is established in the vicinity which may make the TRUE Block Scale site unsuitable. Hence, a new test site may be necessary to find for SWIW tests with synthetic groundwater.

6 References

Andersson P, Wass E, Holmqvist M, Fierz T, 2000. TRUE Block Scale Project, Tracer tests Phase B, SKB IPR-00-29, Svensk kärnbränslehantering AB.

Andersson P, Byegård J, Dershowitz B, Doe T, Hermanson J, Meier P, Tullborg E L, Winberg A, 2002a. Final report of the TRUE Block Scale project. 1. Characterisation and model development. SKB TR-02-13, Svensk kärnbränslehantering AB.

Andersson P, Byegård J, Winberg A, 2002b. Final report of the TRUE Block Scale project. 2. Tracer tests in the block scale. SKB TR-02-14, Svensk kärnbränslehantering AB.

Andersson P, Gröhn S, Nordqvist R, Wass E, 2004. TRUE Block Scale continuation project. BS2B pretests. Crosshole interference, dilution and tracers tests, CPT-1 – CPT-4. SKB IPR-04-25, Svensk kärnbränslehantering AB.

Byegård J, Skarnemark G, Skålberg M, 1995. The use of some ion-exchange sorbing tracer cations in in situ in high saline groundwaters, Mat. Res. Soc. Symp. Proc. 353, 1077–1084.

Byegård J, Johansson H, Skålberg M, Tullborg E-L, 1998. The interaction of sorbing and non-sorbing tracers with different Äspö rock types. Sorption and diffusion experiments in the laboratory scale. SKB TR-98-18, Svensk kärnbränslehantering AB.

Byegård J, Ramebäck H, Widestrand H, 2002. TRUE-1 Continuation project. Use of radon concentrations for estimation of fracture apertures – Part 1: Some method developments, preliminary measurements and laboratory experiments. SKB IPR-02-68, Svensk kärnbränslehantering AB.

Haggerty, 1999. Application of the multirate diffusion approach in tracer test studies at Äspö HRL, SKB R-99-62, Svensk kärnbränslehantering AB.

Holmqvist M, Andersson P, Byegård J, Trick T, Fierz T, Eichinger L, Scholtis A, 2002. TRUE Block Scale Project detailed characterisation stage, Test of new possible non-reactive tracer, Experimental description and evaluation, SKB IPR-02-71, Svensk kärnbränslehantering AB.

Li YH, Gregory S, 1974. Diffusion of ions in sea water and in deep sea sediments. Geochim. et Cosmochim. Acta.

Moreno L, Neretniks I, Klockars C-E, 1983. Evaluation of some tracer tests in the granitic rock at Finnsjön. SKB TR 83-38, Svensk kärnbränslehantering AB.

Neretnieks I, 2002. Using 222Rn to assess the fracture apertures in fractured rocks, in Proceedings of the International Groundwater Symposium, LBNL, Berkley Calicornia, March 25–28.

Nordqvist R, 2007. Evaluation and modelling of SWIW tests performed within the SKB site investigation programme. SKB report in prep.

Skagius K, Neretnieks I, 1986. Porosities and diffusivities of some nonsorbing species in crystalline rock, Water Resources Res. 22(3) 389–398.

Voss C I, 1984. SUTRA – Saturated-Unsaturated Transport. A finite element simulation model for saturated-unsaturated fluid-density-dependent ground-water flow with energy transport and chemically-reactive single-species transport. U.S. Geological Survey Water-Resources Investigations Report 84-4369.

Winberg A, Andersson P, Hermanson J, Byegård J, Cvetkovic V, Birgersson, L 2000, Äspö Hard Rock Laboratory. Final report of the first stage of the tracer retention understanding experiments, SKB TR-00-07, Svensk kärnbränslehantering AB.

Appendix A

Extended proposal for chemicals and tracers to be used in the synthetic groundwater experiment, discussions concerning the data are presented in the text in the previous chapters. The original proposal is presented in Table 4-8.

Chemical	Purity	g/litre of water	Cost [a]	Contamination in chemical (ppm)					Contamination in synth. groundwater (ppb)							Cost ground water (SEK per litre)
				Cl^-	Na^+	Ca^{2+}	SO_4^{2-}	K^+	Cl^-	Na^+	Ca^{2+}	SO_4^{2-}	K^+	He	Rn-222	
Li_2CO_3	≥ 99.99%	2.91	1,870 SEK per 100 g	10	10	5	54	50	29	29	15	150	29			54
HNO_3	≥ 69% [1]	17.75	3,500 SEK per 4,200g	0.3	0.01	0.01	15	0.05	5	0.2	0.2	0.9	0.2			15
Mg	99.98%	0.79	1,200 SEK per 1,000g	5	30	7	4	5	4	24	6	4	4			4
H_2SeO_4	40% [1]	1.62	1,513 SEK per 140 g	100	86.8	100	100	4.5	160	140	6	160	7			18
$RbNO_3$	99.99%	0.048	2,081 SEK per 10g	100	0.47	100	10	100	5	0.02	5	5	5			10
Total									205	190	31	320	45	Very low	Detection limit: 0.03 Bq/l	100
Natural groundwater									5.4E+6	1.7E+6	1.3E+6			5–15 ml/l	400 Bq/l	
Dynamic range									3E+4	9E+3	4E+4	1E+3	3E+2	Very high	1E+4	
D_w (m^2/s)									2.0E–9	1.3E–9	7.9E–10	1.1E–9	2.0E–9	5.8E–9	1.1E–9	
K_d (m^3/kg)									0	4E–6	4E–5	0	2E–4	0	0	